

1970

# Fatigue consideration of unsymmetrical plate girders

Siamak Parsanejad

*Lehigh University*

Follow this and additional works at: <https://preserve.lehigh.edu/etd>



Part of the [Civil Engineering Commons](#)

---

## Recommended Citation

Parsanejad, Siamak, "Fatigue consideration of unsymmetrical plate girders" (1970). *Theses and Dissertations*. 3823.  
<https://preserve.lehigh.edu/etd/3823>

This Thesis is brought to you for free and open access by Lehigh Preserve. It has been accepted for inclusion in Theses and Dissertations by an authorized administrator of Lehigh Preserve. For more information, please contact [preserve@lehigh.edu](mailto:preserve@lehigh.edu).

FATIGUE CONSIDERATION  
OF UNSYMMETRICAL PLATE GIRDERS

by

Siamak Parsanejad

A Thesis  
presented to the Graduate Committee  
of Lehigh University  
in candidacy for the Degree of  
Master of Science  
in  
Civil Engineering

Lehigh University

1970

CERTIFICATE OF APPROVAL

This thesis is accepted and approved in partial fulfillment  
of the requirement of the degree of Master of Science.

5/8/70  
(Date)

Alexis Ostapenko

Dr. Alexis Ostapenko  
Professor in Charge

David A. VanHorn

Dr. David A. VanHorn, Chairman  
Department of Civil Engineering

### ACKNOWLEDGEMENTS

The work described in this thesis was conducted at Fritz Engineering Laboratory, Department of Civil Engineering, Lehigh University, Bethlehem, Pennsylvania. Dr. Lynn S. Beedle is Director of the Laboratory and Dr. David A. VanHorn is Chairman of the Civil Engineering Department.

The study forms a part of Project 328 entitled "Ultimate Strength of Unsymmetrical Plate Girders". The project is sponsored financially by the American Iron and Steel Institute, the Pennsylvania Department of Highways, Bureau of Public Roads (Department of Transportation), and the Welding Research Council. Technical guidance has been provided by the Welding Research Council Subcommittee for Welded Plate Girders (Mr. M. Deuterman, Chairman) and by the Task Group of this subcommittee (Messrs. C. A. Zwissler and L. A. Daniels, Consecutive Chairmen).

Dr. A. Ostapenko supervised the work of this thesis. The author owes a special debt of gratitude to him for his advice, critical review, and encouragement.

The author wishes to express his appreciation for the assistance and information provided by Dr. B. T. Yen and Mr. J. S. Huang. Thanks are extended to Mr. G. Scott for the use of Bethlehem Steel Computer facilities.

Mrs. Jane L. Lenner typed the complete manuscript with great care, and Mrs. Sharon Balogh prepared the drawings. Their cooperation is appreciated.

TABLE OF CONTENTS

	<u>Page</u>
<b>ABSTRACT</b>	1
<b>1. INTRODUCTION</b>	2
<b>2. METHOD OF ANALYSIS</b>	6
<b>2.1 Plate Bending Stresses</b>	6
<b>2.2 Web Deflections and Stresses         along Stiffeners</b>	7
<b>2.3 Web Deflections and Stresses         along Flanges</b>	14
<b>3. SPECIALIZATION OF THE METHOD AND MODIFICATION     OF BOUNDARY CONDITIONS</b>	17
<b>3.1 Stresses at Stiffeners</b>	17
<b>3.2 Stresses at Flanges</b>	20
<b>3.3 Selection of Loading Range         for Stress Computation</b>	21
<b>4. DESIGN CONSIDERATIONS</b>	26
<b>4.1 Previous Work</b>	26
<b>4.2 Effect of Initial Web Deflection</b>	27
<b>4.3 Effect of the Change in the Initial Web         Deflection Pattern due to Overload</b>	28
<b>4.4 Effect of Slenderness Ratio</b>	29
<b>4.5 Test Results for Unsymmetrical Girders</b>	31
<b>4.5.1 Stresses at Flanges and             Horizontal Stiffeners</b>	32
<b>4.5.2 Stresses at Transverse Stiffeners</b>	32
<b>4.5.3 Summary of the Results</b>	33
<b>5. SUMMARY, CONCLUSIONS, AND RECOMMENDATIONS</b>	35
<b>TABLE</b>	38
<b>FIGURES</b>	39
<b>REFERENCES</b>	53
<b>VITA</b>	54

ABSTRACT

Static test results of two full-scale unsymmetrical plate girder specimens are used for the analysis of the web stresses which are expected to develop in a girder under repeated loading. The significance of these stresses for the fatigue life of unsymmetrical plate girders is evaluated on the basis of an approximate S-N relationship previously obtained for symmetrical girders. A method is described for calculating the plate bending stresses caused by the change in lateral deflection of the web. The modified slenderness ratio  $\beta_u = \frac{2y}{h}$  of the web plate of unsymmetrical plate girders is proposed as a tentative criterion for limiting the web slenderness. Numerical value for  $\beta_u$  is recommended to be the same as that given for the slenderness ratio  $\beta = \frac{b}{h}$  of symmetrical plate girders; it is a function of the yield stress of the web. It is also found that the load history of the panel influences its fatigue strength. A study of the effect of certain geometrical as well as loading parameters on the fatigue strength of plate girders is recommended in order to refine this criterion.

## 1. INTRODUCTION

Unsymmetrical plate girders, that is, girders whose neutral axis is not at the mid-depth of the web plate, are used in many types of structures. Examples of these are orthotropic and composite deck bridges (Fig. 1). Since these structures are subjected to repeated loading, some limiting criteria are needed to preclude development of fatigue cracks during the expected bridge life.

Although substantial research on the fatigue strength of plate girders has been conducted<sup>(1,2,3,4,5)</sup>, all of this dealt with symmetrical plate girders, that is, girders with flanges of equal areas and, consequently, with the centroidal axis at mid-depth.

An important type of fatigue failure which is unique to plate girders is the development of cracks due to the lateral back-and-forth movement of the web plate during the application and removal of loading. As the web plate deflects laterally under an increasing load, bending stresses are induced in the web at its edges since the edges are restrained from rotation by the flanges or stiffeners to which the web is rigidly attached. These stresses may lead to the development of fatigue cracks if the load is re-applied a sufficient number of times.

This phenomenon has been to some extent investigated experimentally. It was observed that the web deflection pattern and consequently the stress variation due to a repeatedly applied load was the same as due to a statically applied load. Hence, the stresses

were measured in almost all cases by applying the load statically.

The available test results were then used to obtain an approximate S-N curve, the stress range versus the number of loading cycles required to develop a crack<sup>(1,4)</sup>. The maximum initial out-of-plane deflection  $w_i$  and the slenderness ratio  $b/h$  for which no cracks had been observed were proposed as limiting design criteria<sup>(2,4)</sup>.

Many plate girders, especially bridge girders, are unsymmetrical with a larger portion of the web being in tension or, in some cases, in compression. No fatigue tests have been conducted on such girders, and the only source of information on lateral web deflections of these girders that can be utilized for a study of the web bending stresses are the two full-scale unsymmetrical plate girder specimens tested under static loading and described in Ref. 6. The purpose of the study described here was to investigate the development of these stresses and to evaluate their significance on the basis of the approximate S-N relationship for symmetrical girders mentioned above<sup>(1,3)</sup>.

More refined methods than previously published<sup>(1)</sup> of calculating web bending stresses at stiffeners (transverse and horizontal) and at flanges were developed and are presented here.

In the course of this study it became apparent that more extensive static test deflection measurements of the girder web than originally taken would have substantially contributed to the accuracy of the computations. Another factor which was recognized in this

study as important in the correlation of static test data with the fatigue strength is the necessity of taking deflection measurements not only during loading to the ultimate load and unloading, but also during a reloading cycle, and, if reloading was not originally planned for static load studies, introducing such reloading cycle or cycles.

The points of the S-N curve of Ref. 1 were recalculated using the new method. Two data points were added in order to establish a better defined band (Fig. 2)<sup>(3)</sup>. Based on this improved S-N relationship the fatigue life of unsymmetrical plate girders was then estimated from the web plate bending stresses.

It was observed that the amount of the lateral back-and-forth movement of the web, when the web is subjected to a certain load range, was influenced by its Maximum Past Load (MPL)\*, especially, when MPL had been appreciably larger than the buckling value of the web plate. The effect of MPL is explained and a recommendation regarding its use is made.

Using the available information, a tentative criterion for the limiting slenderness of the web of unsymmetrical plate girders is recommended. This is the modified slenderness ratio defined by  $\beta_u = \frac{2y_c}{h}$ . Where  $y_c$  is the portion of the web under compression and  $h$  is the thickness of the web. The numerical limiting values of  $\beta_u$  are given as a function of the yield stress of the web.

---

\* "Maximum Past Load" (MPL) of a panel refers to the highest load to which the panel has been subjected in the past.

Finally, because the present limiting criteria are very conservative, recommendations are made for further research to refine them.

## 2. METHOD OF ANALYSIS

### 2.1 Plate Bending Stresses

Upon the application of load to plate girder, plate bending stresses, caused by a change in the initial deflection pattern, are induced in the web. For loads smaller than the buckling value, the change in deflection pattern is of relatively little significance.

However, for loads substantially greater than the buckling value, the change in deflection pattern becomes quite pronounced. This change in deformation pattern results in plate bending stresses which are usually the highest at the edges where the stiffener or the flange restrains the plate from rotation. It has been shown that primarily the web plate bending stresses are responsible for the fatigue crack development<sup>(1)</sup>. Thus, it becomes necessary to determine the magnitude and distribution of these stresses at the edges.

In the following sections, a method of analysis for bending stresses at stiffeners and flanges is presented. This method is more accurate and more general than those used by other researchers<sup>(1,4)</sup>.

The process for computing the stresses may be summarized in the following three steps:

- 1) Deflection of the plate is generalized in the direction perpendicular to the boundary by polynomials passing through the measured deflection points.

2) Boundary conditions controlled by the elastic properties of the stiffener or flange are imposed to solve for the unknown coefficients.

3) The polynomials, with now known coefficients, are then used to obtain the curvatures for computing stresses.

## 2.2 Web Deflections and Stresses Along Stiffeners

As stated above, the plate bending stresses along the stiffener are generated as a result of resistance by the stiffener to the rotation forced upon it by the web. Solution for the plate bending stresses is obtained by requiring that the equilibrium of moments and the compatibility of rotations at the stiffener-to-web junction be satisfied.

These conditions are shown in Figs. 3b and 3c. Location of the points where plate deflection is measured and of the coordinate axes are given in Fig. 3a. Because the stiffener together with a portion of the web inclosed by the stiffener and the weld has much higher rigidity relative to the web plate, a constant slope is assumed for the distance  $2e$  between the toes of the welds on the two sides of the stiffener. Also, because of the high resistance of the stiffener against lateral deflection, it may be assumed that the stiffener remains straight and thus  $w = 0$  for points at the centerline of the stiffener. The validity of the latter assumption

is discussed in detail in Ref. 1 (Page 12). As a result of these assumptions, the deflections at the toes of the weld on the left and the right sides of the stiffener are given respectively by

$$w_{tl} = -e \cdot \theta \quad (2.1a)$$

$$w_{tr} = e \cdot \theta \quad (2.1b)$$

where  $e$  is a positive quantity representing the distance from the toe of the weld to the centerline of the stiffener and  $\theta$  is the angle of twist of the stiffener. With the angle between the web and the stiffener remaining the same before and after loading, the compatibility condition is

$$\theta = -\frac{\partial w_l}{\partial x} \Big|_{x=-e} = -\frac{\partial w_r}{\partial x} \Big|_{x=e} \quad (2.2)$$

where  $w$  is the change in the out-of-plane deflection of the web. Deflection  $w$  is obtained as the difference between the deflections under the maximum and minimum loads

$$w = w_{\max} - w_{\min} \quad (2.3)$$

It is important to keep in mind that deflections on both sides of the stiffener are referred to the same system of coordinate axes. Substitution of the compatibility condition of Eq. (2.2) in Eq. (2.1) gives

$$w_{tl} = e \frac{\partial w}{\partial x} \Big|_{x=-e} \quad (2.4a)$$

$$w_{tr} = -e \frac{\partial w}{\partial x} \Big|_{x=e} \quad (2.4b)$$

Next, the equilibrium equation for the stiffener-to-web junction, at the toe of the weld, is derived. Designating the twisting moment in the stiffener by  $m_t$  and the plate bending moments to the left and to the right of the stiffener by  $M_{xl}$  and  $M_{xr}$ , respectively, the equation of equilibrium is expressed according to Fig. 3b by

$$m_t = \left[ M_{xr} - V_{xr} e \right]_{x=e} - \left[ M_{xl} + V_{xl} e \right]_{x=-e} \quad (2.5)$$

$V_{xr}$  and  $V_{xl}$  are the shear forces at the toe of the welds to the right and to the left of the stiffener, respectively.

For the stiffener, the relationship between the twisting moment and the twisting angle is given by (8, p.163).

$$m_t = EI_w \frac{\partial^4 \theta}{\partial y^4} - GK_t \frac{\partial^2 \theta}{\partial y^2} \quad (2.6)$$

where  $EI_w$  and  $GK_t$  are the warping and St. Venant (pure torsion) rigidities of the stiffener. Since the stiffener consists of two narrow rectangles, the warping rigidity becomes negligible and Eq. (2.6) is simplified to\*

---

\* The negligibility of  $I_w$  should be studied if stiffeners are of some other shape.

$$m_t = -GK_t \frac{\partial^2 \theta}{\partial y^2} \quad (2.7)$$

Neglecting the effect of the portion of the web inclosed by the weld on the torsional rigidity of the stiffener, the torsional constant  $K_t$  for a two sided rectangular stiffener is\*

$$K_t = (2 b_s + h) \frac{t_s^3}{3}$$

where:

$b_s$  = width of a single stiffener

$t_s$  = thickness of the stiffener

$h$  = thickness of the web

The plate bending moments are given by (7)

$$M_x = -D \left[ \frac{\partial^2 w}{\partial x^2} + v \frac{\partial^2 w}{\partial y^2} \right] \quad (2.8)$$

where:

$$D = \frac{Eh^3}{12(1-v^2)} = \text{plate flexural rigidity}$$

$h$  = web plate thickness

$E$  = modulus of elasticity (Young's modulus)

$v$  = Poisson's ratio

The effect of curvature in the direction parallel to the stiffener,  $\frac{\partial^2 w}{\partial y^2}$ , on the bending moment in the direction perpendicular to the

---

\* In a more refined analysis the weld and the neglected portion of the plate may be included. Also, a different formula should be used if stiffeners are of some other shape.

stiffener,  $M_x$ , has been shown to be negligible for points close to the stiffener<sup>(1, p. 12)</sup>. Thus, this effect should be even smaller for points at the toe of the weld. Therefore, the term  $\nu \frac{\partial^2 w}{\partial y^2}$  in Eq. (2.8) may be neglected. The expression for the plate bending moment is then reduced to

$$M_x = -D \frac{\partial^2 w}{\partial x^2} \quad (2.9)$$

The shear force in terms of the deflection of the web is given by<sup>(7)</sup>

$$V_x = -D \left[ \frac{\partial^3 w}{\partial x^3} + (2-\nu) \frac{\partial^3 w}{\partial x \partial y^2} \right] \quad (2.10)$$

Substitution of Eqs. (2.2), (2.7), (2.9), and (2.10) into Eq. (2.5) yields one of the boundary conditions at the stiffener

$$\left[ \frac{GK_t}{D} - (2-\nu)e \right] \frac{\partial^3 w_l}{\partial x \partial y^2} \Big|_{x=-e} - (2-\nu)e \frac{\partial^3 w_r}{\partial x \partial y^2} \Big|_{x=e} = \\ \left[ e \frac{\partial^3 w_r}{\partial x^3} - \frac{\partial^2 w_r}{\partial x^2} \right]_{x=e} + \left[ e \frac{\partial^3 w_l}{\partial x^3} + \frac{\partial^2 w_l}{\partial x^2} \right]_{x=-e} \quad (2.11)$$

As shown in Fig. 3c, the deflected shape of the web for a particular level of  $y$  is expressed on each side of the stiffener by a polynomial passing through the points given by the measured deflections and the points defined by Eq. (2.4). The order of each polynomial is equal to the number of measured points on its

respective side plus one. For the girder shown in Fig. 3a, with  $n$  and  $m$  columns of measured points on the left and on the right sides of the stiffener, respectively, the polynomials for the  $j$ -th level of  $y$  are of the following general form:

$$(w_j)_l = l_{j,0} + l_{j,1}x + l_{j,2}x^2 + \dots + l_{j,n+1}x^{n+1} \quad (2.12a)$$

$$(w_j)_r = r_{j,0} + r_{j,1}x + r_{j,2}x^2 + \dots + r_{j,m+1}x^{m+1} \quad (2.12b)$$

where  $j$  refers to the  $j$ -th row of deflection readings and varies from 1 to  $s$ ;  $l$  and  $r$  are the unknown coefficients of the two polynomials on the left and right sides, respectively. It should be noted that on both sides  $x$  refers to the same coordinate system and appropriate signs should be used, and that Eqs. (2.12) pertain to the plate only and do not cover the distance  $2e$  between the toes of the welds.

Now the solution of the problem depends on the determination of the  $(s) \cdot (m+n+4)$  unknown constants  $l$  and  $r$ . The solution proceeds by generating a set of simultaneous linear equations.

$(n+1)$  equations are produced for each row of the measured points by substituting  $n$  deflections to the left of the stiffener and the deflection given by Eq. (2.4a) into Eq. (2.12a). Repetition of this process for each of the  $s$  rows of measured points gives  $(s) \cdot (n+1)$  equations. Similarly, the points to the right of the stiffener, Eq. (2.4b), and Eq. (2.12b) yield  $(s) \cdot (m+1)$  equations which together with the previous equations result in  $(s) \cdot (m+n+2)$  equations. The

remaining (2.s) equations are obtained from the following boundary conditions:

B.C.1. The continuity of the slope in the x-direction at the toes of the welds, that is,

$$\frac{\partial w_l}{\partial x} \Big|_{x=-e} = \frac{\partial w_r}{\partial x} \Big|_{x=e} \quad (2.13)$$

B.C.2. Equilibrium of moments, Eq. (2.11).

Imposition of B.C.2, however, involves the second derivative of the deflection along the y-axis. Here, instead of using continuous derivatives, the finite difference formulation is employed. Using variable spacing  $c_1$  to  $c_{s+1}$  (Fig. 3a), the following expression is derived:

$$\left( \frac{\partial^3 w}{\partial x \partial y^2} \right)_j = 2 \frac{c_{j+1} \left( \frac{\partial w}{\partial x} \right)_{j-1} - (c_j + c_{j+1}) \left( \frac{\partial w}{\partial x} \right)_j + c_j \left( \frac{\partial w}{\partial x} \right)_{j+1}}{c_j c_{j+1} (c_j + c_{j+1})} \quad (2.14)$$

A substitution of Eq. (2.14) and of the continuous second and third derivatives of the deflection functions of Eqs. (2.12a) and (2.12b) into Eq. (2.11) for each location  $j$  gives the equations needed to satisfy B.C.2.

Using the deflection functions of Eqs. (2.12), now with known coefficients, the curvatures, at some discrete points along

the stiffener, can be evaluated simply by taking second derivatives of these functions. Then, the bending stresses in the plate are computed from

$$\sigma_{bx} = - \frac{Eh}{2(1-\nu^2)} \frac{\partial^2 w}{\partial x^2} \quad (2.15)$$

where  $\frac{\partial^2 w}{\partial x^2}$  is the second derivative of the  $w$  function of Eqs. (2.12).

### 2.3 Web Deflections and Stresses Along Flanges

Determination of the plate bending stresses along flanges is essentially a special case of the formulation outlined in Section 2.2. As can be seen in Fig. 4a, a flange may be treated as a stiffener with the web plate connected on one side only. By dropping the  $M_{xr}$  and  $V_{xr}e$  terms from Eq. (2.5) the equilibrium relationship for the flange-to-web junction is derived

$$m_t = - \left[ M_x + V_x e \right]_{x=-e} \quad (2.16)$$

Equation (2.16) can also be formulated directly from Fig. 4b where the equilibrium condition at the flange-to-web junction is sketched.

Figure 4c illustrates the compatibility of the angle of twist of the flange and the slope of the web plate, which, assuming a rigid flange-to-web connection, can be expressed by

$$\theta = - \left. \frac{\partial w}{\partial x} \right|_{x=-e} \quad (2.17)$$

Here again, because the flange and the portion of the web inclosed by the welds have higher rigidity relative to the web plate, a constant slope is assumed for the distance from the centroid of the flange to the toe of the weld.

Since the overall bending moment of the girder produces an axial force in the flange, the twisting moment expression of Eq. (2.3) is modified to (8, p.163).

$$m_t = - (GK_t + P r_o^2) \frac{\partial^2 \theta}{\partial y^2} \quad (2.18)$$

where:

$P$  = the axial force in the flange, positive when tensile

$r_o = \frac{I_x + I_z}{A_f}$  = polar radius of gyration of the flange

$A_f$  = area of the flange

$I_x$  = moment of inertia of the flange about its centroidal x-axis

$I_z$  = moment of inertia of the flange about its centroidal z-axis

$$K_t = b_f t_f^3 / 3$$

$b_f$  = width of the flange

$t_f$  = thickness of the flange

Employing the previous modifications in the derivation outlined in Section 2.2, the boundary condition for the flange-to-web junction becomes

$$\left[ \frac{GK_t + P r_o^2}{D} - (2-\nu)e \right] \frac{\partial^3 w}{\partial x \partial y^2} \Big|_{x=-e} = e \frac{\partial^3 w}{\partial x^3} + \frac{\partial^2 w}{\partial x^2} \Big|_{x=-e} \quad (2.19)$$

Then, following a procedure similar to the procedure explained for the stiffener-to-web junction, the deflection equations are obtained and the bending stresses computed.

### 3. SPECIALIZATION OF THE METHOD AND MODIFICATION OF BOUNDARY CONDITIONS

Application of the method described in Section 2.2 for calculating plate bending stresses at a stiffener requires deflection measurements to the left and to the right of the stiffener. For some panels of the two specimens of Ref. 6 one column of deflection readings in the neighboring panel was obtained and the method could be employed for them. However, for most test panels no deflection readings were taken on the neighboring panel side of the stiffener because of the interference with diagonal reinforcement bars and the method had to be modified. A fixed boundary was assumed at the stiffener and the accuracy of this assumption was investigated by comparing the resultant bending stresses with those obtained by the more general method\*.

#### 3.1 Stresses at Stiffeners

##### Transverse Stiffeners

The first step in calculating plate bending stresses according to the method of Section 2.2 is the selection of the order of the polynomials. For the test panels with one column of deflection measurements in the neighboring panel, the configuration sketched in

\* For the sake of distinguishing the method of analysis presented in this chapter from the simplified methods described later in this chapter, this method will be designated as the "general method".

Fig. 5 with three columns of deflection readings in the test panel was used, and the polynomials of Eqs. (2.12) were specialized to

$$(w_j)_\ell = \ell_{j0} + \ell_{j1} x + \ell_{j2} x^2 + \ell_{j3} x^3 + \ell_{j4} x^4 \quad (3.1a)$$

$$(w_j)_r = r_{j0} + r_{j1} x + r_{j2} x^2 \quad (3.1b)$$

The unknown coefficients  $\ell_{ji}$  and  $r_{ji}$  were determined by the approach explained in Section 2.2. The bending stress at the toe of the weld was then given by Eq. (2.15) with  $x = -e$ .

Accuracy of the method was checked by comparing the computed stresses with the experimental results. The bending stresses for the points at which strain gages were located were computed from the weighted average curvature over the gage lengths and compared with the stresses actually measured by the gage. The equation for the weighted average gage stress is

$$\sigma_g = \frac{-Eh}{2(1-\nu^2)} \frac{\int_{x_1}^{x_2} \frac{d^2 w}{dx^2} dx}{x_2 - x_1} \quad (3.2)$$

where  $x_1$  and  $x_2$  are the x-coordinates of the gage ends. In Fig. 6, the calculated and measured stresses at stiffeners of the two symmetrical

plate girders (girders F3 and F9 of Ref. 3)\* are shown by solid lines and solid dots, respectively. For both girders, the theoretical and experimental results can be seen to correlate well.

To check the assumption of fixed boundary at the stiffeners, the bending stress distribution along the stiffeners with deflection readings on neighboring panels were calculated treating the web as a cantilever. A graphical representation of this model is shown in Fig. 7 where three measured points are used to define the deflected shape of the web. Here again, because the stiffener together with the portion of the web enclosed by the stiffener and the welds has much higher rigidity relative to the web, the point of fixity was assumed at the toe of the weld. This model will be referred to as "Boundary Condition 1" or in an abbreviated form as "B.C.1".

In general, the bending stresses obtained assuming fixity at the toe, as shown in Fig. 8a, were close to those obtained by allowing rotation \*\*. However, in the region of the maximum bending stresses along a stiffener, B.C.1 consistently gave higher values.

\* For checking the method, some test results of symmetrical plate girders tested at Lehigh University were used because the strain gages were located closer to the toe of the weld than in the unsymmetrical specimens of Ref. 6 and thus the check was of greater significance.

\*\* This accuracy may have been good only because the stiffeners of the two girder specimens were proportionally larger than those normally used in practice.

To compensate for the overestimate, another model was selected (B.C.2) by moving the point of fixity to the face of the stiffener (Fig. 7). As illustrated in Fig. 8b, this new assumption gave a closer estimate of the maximum bending stress to that computed by the general method.

Based on the above findings, B.C.2 (fixity at the face of the stiffener) was used for bending stress computation. This was done in order to make possible the computation of bending stresses at the stiffeners with no deflection readings in the neighboring panel.

#### Longitudinal Stiffeners

Investigation of the plate bending stresses along longitudinal stiffeners showed that the simplification of assuming the plate to be fixed at the weld toe (B.C.1) or at the face of the stiffener (B.C.2) led to a considerable inaccuracy. This is indicated in Fig. 9 where B.C.2 gives substantially higher values in the region of maximum bending stresses than the general method. Therefore, the general method was consistently used for the determination of bending stresses along longitudinal stiffeners.

#### 3.2 Stresses at Flanges

For computing stresses along flanges, the configuration shown in Fig. 10 was employed. Accordingly, the polynomial of Eq. (2.12a) was modified to

$$w = l_{j_0} + l_{j_1} x + l_{j_2} x^2 + l_{j_3} x^3 + l_{j_4} x^4 \quad (3.3)$$

Upon determination of the unknown constants  $l_{j_i}$ , the bending stresses were computed from Eq. (2.15) with  $x = -e$ .

For bending stresses along the flanges, a similar study to that described in Section 3.1 was carried out. The results were, in general, the same as found for the stiffeners, that is, B.C.1 and B.C.2 gave slightly higher and slightly lower stresses, respectively, in the region of maximum bending stress than the general method. A comparison of the bending stress distributions using the general method, B.C.1, and B.C.2 is made in Fig. 11 for a typical flange. For the sake of simplicity, B.C.2 was selected for bending stress computations at flanges.

It should be noted that, although B.C.1 and B.C.2 proved to give acceptable results for the plate bending stress analysis at the flanges and transverse stiffeners of girders of Ref. 6, they are not recommended to be employed unless their accuracy can be checked.

### 3.3 Selection of Loading Range for Stress Computation

The general purpose of fatigue studies is to establish a relationship between the stress range and the number of loading cycles needed to initiate a crack, the S-N curve. In the most of previous fatigue research, the stress range was taken to be directly proportional to the loading range. However, for plate girders, the

stress range of interest here is the change in plate bending stress caused by the change in deformation pattern which is not directly proportional to the loading range; it is some non-linear function of geometry, initial deformations, magnitude of the loads, etc.

In the course of the study, it was observed that the change in the deformation pattern of the web depends on the maximum load to which the web has been subjected in the past, the maximum past load (MPL).

This can be explained by the degree of local plastification of the web under the action of the MPL. As the load increases beyond the buckling value of the panel, the out-of-plane deflection of the panel becomes more and more pronounced, and the deformation pattern changes to conform to the loading condition. In consequence, due to the change in curvature, local yielding occurs at the boundaries of the panel. After unloading, residual stresses form in the plastified zones and restrain the panel from restoring its initial (original) deformation pattern. This change in the initial deformation pattern due to the MPL of the panel may be seen in Fig. 12a where the out-of-plane deflections of the web are plotted under zero loads before and after the girder was subjected to the maximum load. The amount of the change depends on the extent of plastification along the boundaries of the panel and is thus smaller for panels with a smaller MPL. The change becomes much more pronounced if the panel is loaded far beyond its buckling value, possibly close to its ultimate strength where the

yielding appears also at other locations within the panel, for example, along the tension field. This is seen in Fig. 12b where the initial out-of-plane deflection of the web is compared with the out-of-plane deflection of the web after the panel has been loaded to the ultimate and then unloaded. In this case, the new deformation pattern has no resemblance to the initial pattern.

In Fig. 13, a plot of load versus lateral deflection of a point on the web is shown. It is apparent that the change in the lateral deflection of the point under the range of loading specified there is considerably smaller in the second loading cycle than in the first loading cycle. It may also be noted that, upon reapplication of the same loading range, the change in deflection of the point remains nearly the same provided that the maximum load does not exceed the maximum past load (MPL). The loads of 27.5 per cent and 55 per cent of the ultimate load have been used as representative of the minimum and maximum working loads to which a girder may be subjected<sup>(2)</sup>.

In the panels of the two unsymmetrical test girder specimens, because of very high slenderness ratio, local yielding was observed along the boundaries of the panels even at the working load of  $0.55 P_u$ . This is illustrated in Figs. 14, 15, 16, and 17 for panel UG 5.3. Figures 14, 15, and 16 show the contour plots of the initial web deflection, of the lateral web deflection under 140 kips load, and of the change in the lateral web deflection due to

the application of 140 kips load, respectively. The bending stress distributions along the left stiffener for different load ranges are plotted in Fig. 17. Strains larger than the yield strain of the web under the working load are indicated in Fig. 17a by the bending stress stresses larger than the yield stress of the web.

Because of the excessive amount of yielding along the boundaries of the test panels and also because the permanent change in the initial deformation pattern (such as formation of the tension field) could be expected in such slender webs even at the working load, the selection of the deflection range from the first path of loading seemed to be unrealistic. For more accurate analysis of the bending stresses, therefore, it was desirable to have deflection readings during the unloading of the panel after it had been subjected to its working load. Even more desirable would have been readings for subsequent loading cycles. In this study, only the unloading range from the ultimate load was available as the more accurate data than the first loading.

In Fig. 18, the unloading portions of the load versus lateral deflection are plotted for a number of different points on the panels. Although the loading process induced localized yielding and non-linearity, relative linearity is observed for all points during the unloading. Thus, for the stress range calculations, 27.5 per cent of the change in the deflection for the whole unloading range (from the ultimate load to zero load) was used. It should be noted that

because the MPL of the panel was  $P_u$ , that is, the maximum possible, the results are to be regarded as an underestimate of the bending stresses which would normally be induced in the web under repetitive working load.

#### 4. DESIGN CONSIDERATIONS

##### 4.1 Previous Work

Tentative design recommendations based on experimental results have been suggested for symmetrical girders. The factors influencing the formation of the fatigue cracks have been indicated as the following: 1) the magnitude of initial deflections of the web, 2) the magnitude and range of loading, 3) the change of the magnitude of the web deflections under load, 4) the corresponding plate bending stresses, and 5) the properties of the web material in terms of the stress-fatigue life relationship<sup>(2)</sup>.

Conservative limits for slenderness ratio  $\beta$  have been suggested for hybrid<sup>(4)</sup> and homogeneous<sup>(2)</sup> symmetrical girders as 192 for A36 steel and  $36500/\sqrt{F_y}$ <sup>\*</sup>, respectively. Also, a limitation for the initial web deflection has been proposed to be<sup>(4)</sup>

$$\frac{w_i}{t} \leq 1000 \frac{\sigma_{yw}}{E} \quad (4.1)$$

A plot of the relative initial web deflection  $\frac{w_i}{h}$  versus the slenderness ratio  $\frac{b}{h}$  for symmetrical test girders (Fig. 26 of Ref. 2) shows that about one-third of the panels with slenderness ratios greater than 200 and relative initial web deflections less than 2 did not fail when subjected to repeated loading over 2,000,000 cycles.

---

\*190 for A36 steel.

This and a lack of correlation between the bending stress and the slenderness ratio, which was observed in this study (Section 4.5.2), seem to indicate that the slenderness ratio and the relative initial web deflection alone cannot be used as efficient limiting design criteria to preclude fatigue failure. Other geometrical as well as loading parameters should be taken into account.

In this study, the effects of initial web deflection, slenderness ratio, and the change in web deflection pattern under overload on the fatigue strength of girders have been evaluated and presented in the following sections. In the process, the proposed stress computation method was applied to unsymmetrical as well as symmetrical girders.

#### 4.2 Effect of Initial Web Deflection

The relative magnitude of the initial web deflection  $\frac{w_i}{h}$  has been introduced as one of the factors controlling the occurrence of fatigue cracks<sup>(2,4)</sup>. However, as pointed out earlier in Section 3.3, because of the partial plastification of the web plate, the deformation pattern of the web under zero load would be modified in comparison with the initial web deformation pattern if the panel was loaded beyond its buckling value in its past life. It may be thus concluded that the magnitude and pattern of the web plate deflections existing before the girder is loaded may have little significance on the fatigue life. The new deflection pattern which develops after

the maximum past load (MPL) of the girder is reached should be used as the basis. Some of the previous investigators have, in fact, used it as the initial web deflection<sup>(2)</sup>.

The new deflection pattern can be influenced by the actual initial deflection of the web plate. However, as shown in Fig. 12b, in cases where the MPL considerably exceeds the buckling value this effect is negligible. It should be noted that in some panels, in which local plastification does not occur under loads of practical significance, the web is likely to maintain its initial deflection pattern. In this case, the effect of initial deflection on the development of fatigue cracks may be of direct significance. However, for thin web plate girders this is very unlikely.

Therefore, it is tentatively concluded that if the MPL of a panel is sufficiently high to change the deformation pattern of the panel significantly, such as when it exceeds the buckling value, the initial web deflection of the panel cannot be used as a reliable criterion for controlling the occurrence of fatigue cracks.

#### 4.3 Effect of the Change in the Initial Web Deflection Pattern due to Overload

As noted in Sections 3.3 and 4.2, a permanent change in the initial deformation pattern of a web is expected if it is subjected to a load higher than its buckling value. It was also observed that this permanent change in the initial deformation pattern tends to reduce

the amount of the flexing that the web would undergo under a repeated load range. Consequently, an increase in the fatigue strength of a panel may be expected after it is subjected to an overload (MPL), which is higher than the buckling value. It should be noted, however, that since the change in deflection pattern is such as to conform to the type of loading\*, the increase in fatigue strength is possible only if the structure is subjected mainly to the same type of loading all through its expected life. If a panel is to be subjected to different types of loading, its deformation pattern will change each time to conform to the new loading condition. In this case, it is less likely that overloading can improve the fatigue strength.

It may be concluded, then, that overloading of a girder panel is beneficial to its fatigue strength, provided the panel will be, mainly, subjected to the same type of loading throughout its service life.

#### 4.4 Effect of Slenderness Ratio

Because of a lack of sufficient number of test results, it is impossible to directly establish limits of slenderness ratio for unsymmetrical plate girders. Thus, the limit set for symmetrical girders is tentatively recommended, except that the controlling slenderness ratio should be defined somewhat differently.

---

\* "Type of Loading" is defined as a certain combination of shear and moment and may be represented by the ratio  $\frac{M}{Vb}$ .

It has been reported that the fatigue cracks caused by the flexing of the web are usually located in the compressed portion of the web<sup>(1,4)</sup>. This is simply because compression tends to amplify the deflections. On the other hand, the tension, to the other side of the centroidal girder axis, tends to reduce deflections and thereby reduces the possibility of the occurrence of fatigue cracks. It follows, then, that the portion of the web depth under compression should be a more important factor than the full depth in limiting the slenderness of the web in order to inhibit formation of fatigue cracks. On this basis, it is suggested that

$$\beta_u = \frac{2y_c}{h} \quad (4.2)$$

be used as a controlling slenderness ratio rather than the slenderness ratio for the full depth

$$\beta = \frac{b}{h} \quad (4.3)$$

where:

$b$  = web depth

$y_c$  = portion of the web depth under compression

$h$  = web thickness

Equation (4.2) reduces to Eq. (4.3) for symmetrical girders.

The limitation given by Eq. (4.2) should be further investigated for the case of pure shear or where the shear is dominant.

#### 4.5 Test Results for Unsymmetrical Girders

Nine panels of the two unsymmetrical girder specimens (UG 4.2, 4.5, and UG 5.1 to 5.6 of Ref. 6) were analyzed for the plate bending stress distribution at the web boundaries. The results are presented in Table 1.

As discussed in Section 3.3, a load of 27.5 per cent of the unloading range, from the ultimate load to the zero load, was used for the bending stress calculation. Hence, the maximum past load (MPL) of each panel was equal to the ultimate load. However, since girders used in practice are not normally subjected to an overload especially of such a magnitude, their MPL may be assumed equal to their maximum working load  $P_{max}$  and the range of loading to  $P_{max} - P_{min}$ . Consequently, the change in the lateral deflection of 27.5 per cent of the unloading range may be expected to be smaller than the change in deflection due to a loading range of  $P_{max} - P_{min}$  when the MPL is assumed equal to  $P_{max}$ . Also, the web thickness and stiffener sizes of the two test girders were somewhat different than those that would be recommended in practice. For these reasons, the test results of the unsymmetrical plate girder specimens could not be presented as examples of the expected performance of an actual bridge girder. Nevertheless, the observations presented in Sections 4.5.1, 4.5.2, and 4.5.3 can serve to draw some practical conclusions.

It should be kept in mind that a fatigue life of two million cycles of repeated loading is usually recommended as an acceptable

limit in current practice. Thus, a stress of 24 ksi, corresponding to 2,000,000 cycles in Fig. 2, was used as an indicator of the safe or unsafe nature of the calculated bending stresses of the two unsymmetrical plate girders, and the panels are categorized as "safe" (S) or "not safe" (NS) in column 9 of Table 1.

#### 4.5.1 Stresses at Flanges and Horizontal Stiffeners

The maximum bending stresses observed at horizontal stiffeners and flanges in the compressive portion of the web are listed in columns 6 and 7 of Table 1, respectively. For three panels, the highest stress was in the tensile portion of the web (it is given in the brackets). This may be so because shear was the dominant portion of the loading as indicated by term  $\frac{M}{Vb}$ , the ratio of the moment to shear non-dimensionalized by the web depth. Although the maximum stresses observed do not correlate well with the modified slenderness ratio  $\beta_u$ , the fact that the stresses corresponding to  $\beta_u$  of less than 200 are smaller than 24 ksi indicates that the proposed limitation for  $\beta_u$  is conservative.

The stresses at the horizontal stiffener are relatively lower than at the flanges; this is due to the smaller torsional rigidity of the horizontal stiffener and, therefore, smaller rotational restraint of the web.

#### 4.5.2 Stresses at Transverse Stiffeners

The maximum bending stresses observed at the transverse stiffeners in the compression portion of the web are listed in

column 8 of Table 1. Brackets indicate that the highest stress was in the tensile portion of the web. Parentheses indicate that the stress was in the neighborhood of the anchorage of the diagonal reinforcement bar and, therefore, might have been influenced by local disturbances there.

Relatively high stresses occur at most of these stiffeners regardless of the value of the modified slenderness ratio  $\beta_u$ . This may be attributed to the use of large size stiffeners in the test girders and, consequently, greater rotational restraint of the web than may be expected for more conventionally sized stiffeners. It follows, then, that stiffeners with greater rotational rigidity would lead to a reduced fatigue strength of the panel.

#### 4.5.3 Summary of the Results

In summary, the following observations were made:

- 1) Although the proposed limiting  $\beta_u$  was found to be conservative, a lack of correlation between the bending stress and  $\beta_u$  was apparent.
- 2) The stresses at horizontal stiffeners were relatively low.
- 3) Stiffeners with greater rotational rigidity lead to a reduced fatigue strength.

All these seem to confirm the conclusion arrived at earlier that the slenderness ratio and the maximum initial lateral deflection alone, although conservative, cannot be used as efficient limiting design criteria for precluding the development of fatigue cracks. Other factors, such as, the type of loading  $\frac{M}{V_b}$ , aspect ratio  $\alpha$ , relative compressive portion of the web depth  $\frac{y_c}{b}$ , and the geometry of stiffeners should be in some way taken into account.

## 5. SUMMARY, CONCLUSIONS, AND RECOMMENDATIONS

An important type of fatigue failure which is unique to plate girders is the development of cracks due to the flexing of the web plate when the girder is subjected to repeated loading. In an attempt to tentatively study this type of fatigue behavior of unsymmetrical plate girders, static test results of two full-scale unsymmetrical girder specimens were used for the analysis of the web bending stresses. The significance of these stresses for the fatigue strength of the girders was evaluated by basing it on an approximate stress-fatigue life relationship (S-N curve) previously obtained for symmetrical girders.

An improved method was developed for calculating the plate bending stresses caused by the change in the out-of-plane deflections of the web and is described in Chapter 2. The method was specialized in order to make it applicable to the test girder panels as explained in Chapter 3. The results of this study are presented in Chapter 4, where the effects of the initial web deflection, of the slenderness of the web, and of the load history of the panel on its fatigue behavior are discussed.

### Conclusions:

Based on the test results of the two unsymmetrical plate girder specimens and the information available on symmetrical plate girders, the following conclusions can be drawn:

1. The initial web deflection of the panel has little effect, if any, on the occurrence of fatigue cracks if the panel has been subjected to loads greater than the buckling value.
2. The use of large stiffeners tends to reduce the fatigue life of panels.

Recommendations:

It was shown that the design limitations of Refs. 2 and 4, although conservative in most cases, cannot be used as efficient design criteria and that in some cases they may even result in an unsafe design. This is the case, for example, for panels with transverse stiffeners of high torsional rigidity. It was also observed that the load history (maximum past load) of a panel influences its fatigue strength. The following recommendations are made from these findings:

1. A modified slenderness ratio  $\beta_u = \frac{2y_c}{h}$ , where  $y_c$  and  $h$  are the compressive portion and the thickness of the web respectively, is tentatively recommended as a limiting criterion to preclude fatigue cracks in unsymmetrical plate girders. Numerical value of  $\beta_u$  is given as a function of the yield stress of the web

$$\beta_u \leq \frac{36,500}{\sqrt{F_y}} \quad (5.1)$$

Equation (5.1) is the proposed limit on web slenderness ratio  $\beta$  of symmetrical plate girders given in Ref. 2.

2. Fatigue strength of a panel may be increased by overloading if the following are true:

a. The panel is subjected to approximately the same type of loading throughout its expected life.

b. The overload\* exceeds the buckling value of the panel. This requirement is automatically satisfied when the maximum working load ( $P_{max}$ ) of the panel is larger than its buckling value.

Recommendation for Future Research:

The effects of loading as well as of geometrical parameters, such as the ratio of moment to shear non-dimensionalized by the web depth  $\frac{M}{V_b}$ , aspect ratio  $\alpha$ , and the dimensions of the stiffener, on the fatigue strength of the panel should be studied in greater detail in order to arrive at more comprehensive limiting criteria.

---

\* Overload is defined as a load larger than the maximum working load.

TABLE 1: TEST RESULTS OF UNSYMMETRICAL PLATE  
GIRDER SPECIMENS (Ref. 6)

Girder	Panel No.	$\alpha$	$\beta_u$	$\frac{M}{Vb}$	Bending Stress (ksi)			Cate- gory
					HS	F	TS	
UG 4	2	1.15	262	2.35	-	24	32	NS
	4	1.77	346	3.50	-	39	16	NS
	5	0.83	178	2.20	-	8	(33)[38]	NS
UG 5	1	2.40	336	0.90	22	[31]	18	NS
	2	1.55	336	2.40	15	[17]	29[32]	NS
	3	1.97	336	3.70	18	-	26	
	4	2.40	199	3.50	21	-	10[(32)]	S
	5	1.13	199	2.20	15	-	31	NS
	6	2.40	199	0.90	20	[22]	13[18]	S

F Flange

HS Horizontal Stiffener

TS Transverse Stiffener

[ ] Encloses the highest stress when it occurs in tension portion of the web

( ) Encloses the stresses which might have been influenced by local disturbances

S Safe ( $N > 2 \times 10^6$  cycles)

NS Not Safe ( $N < 2 \times 10^6$  cycles)

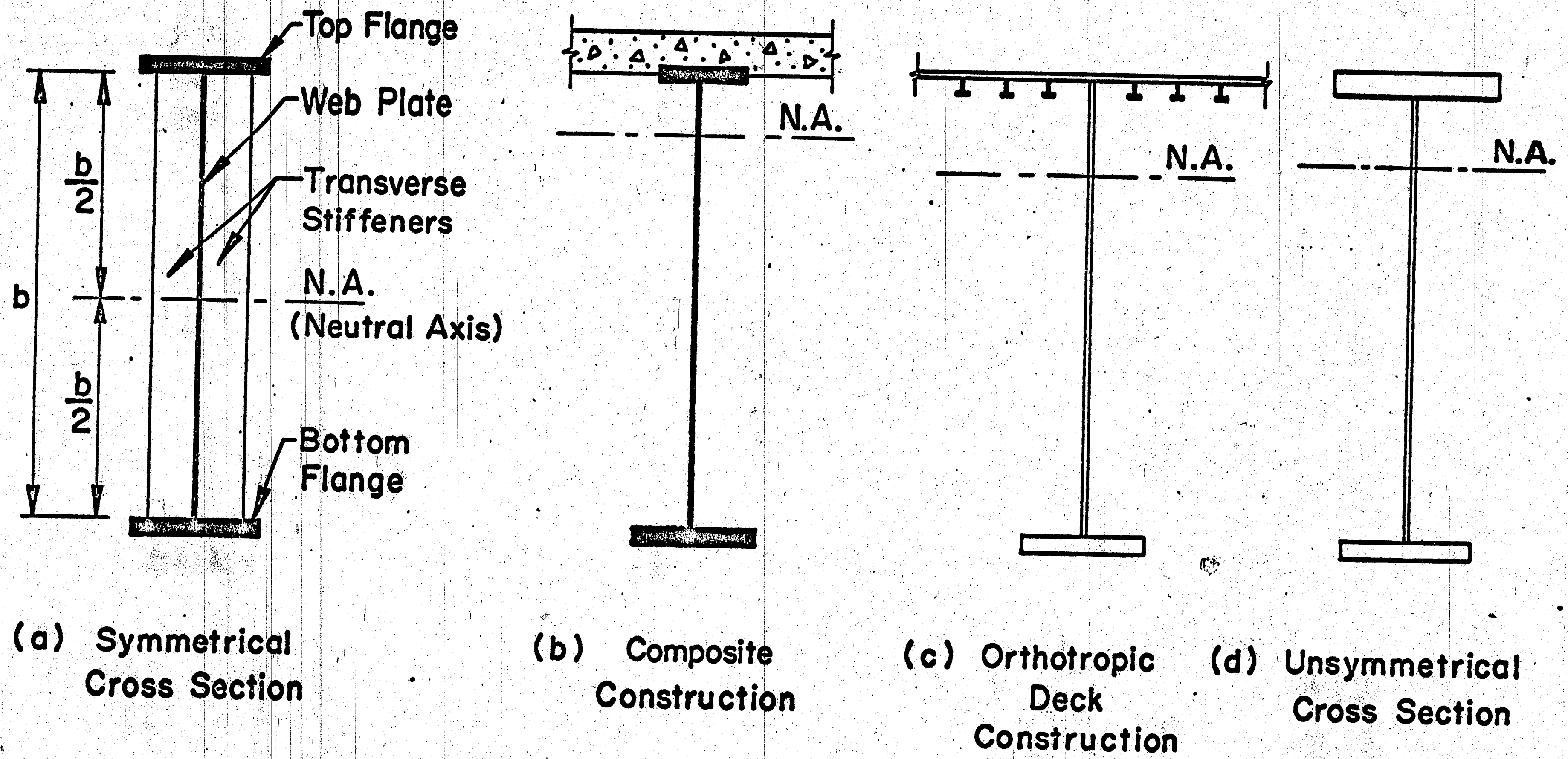


Fig. 1 Symmetrical and Unsymmetrical Girders

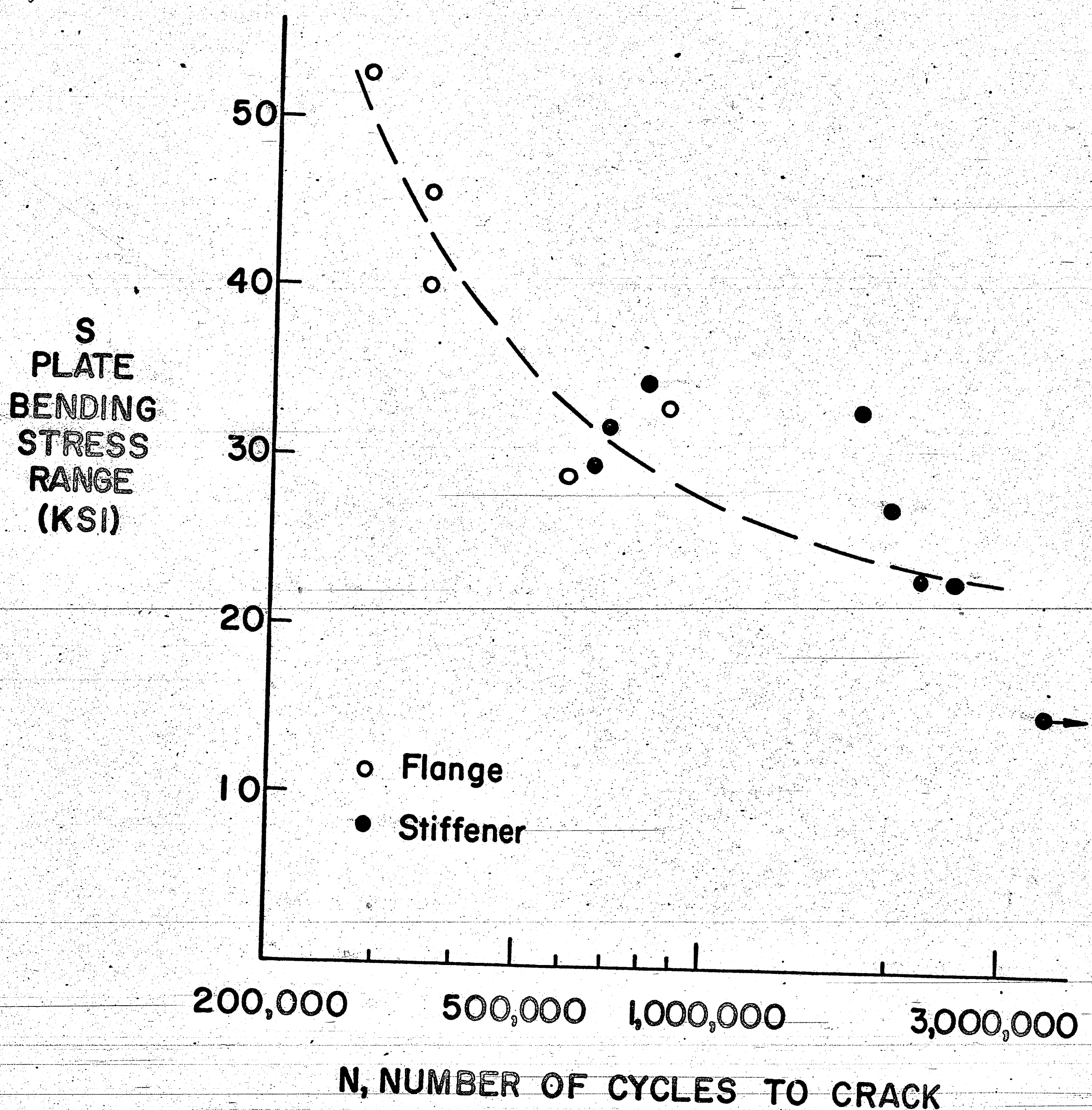
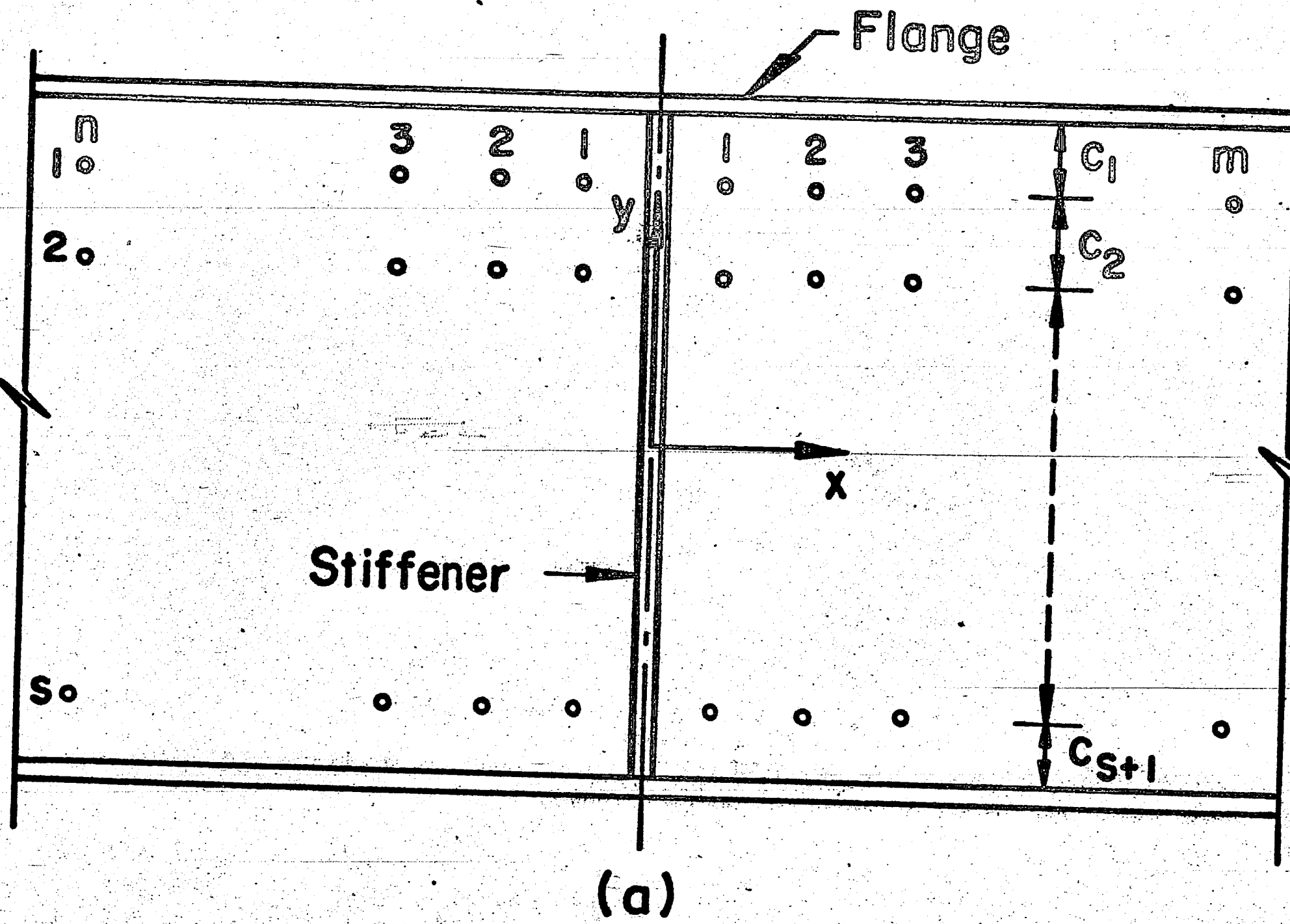
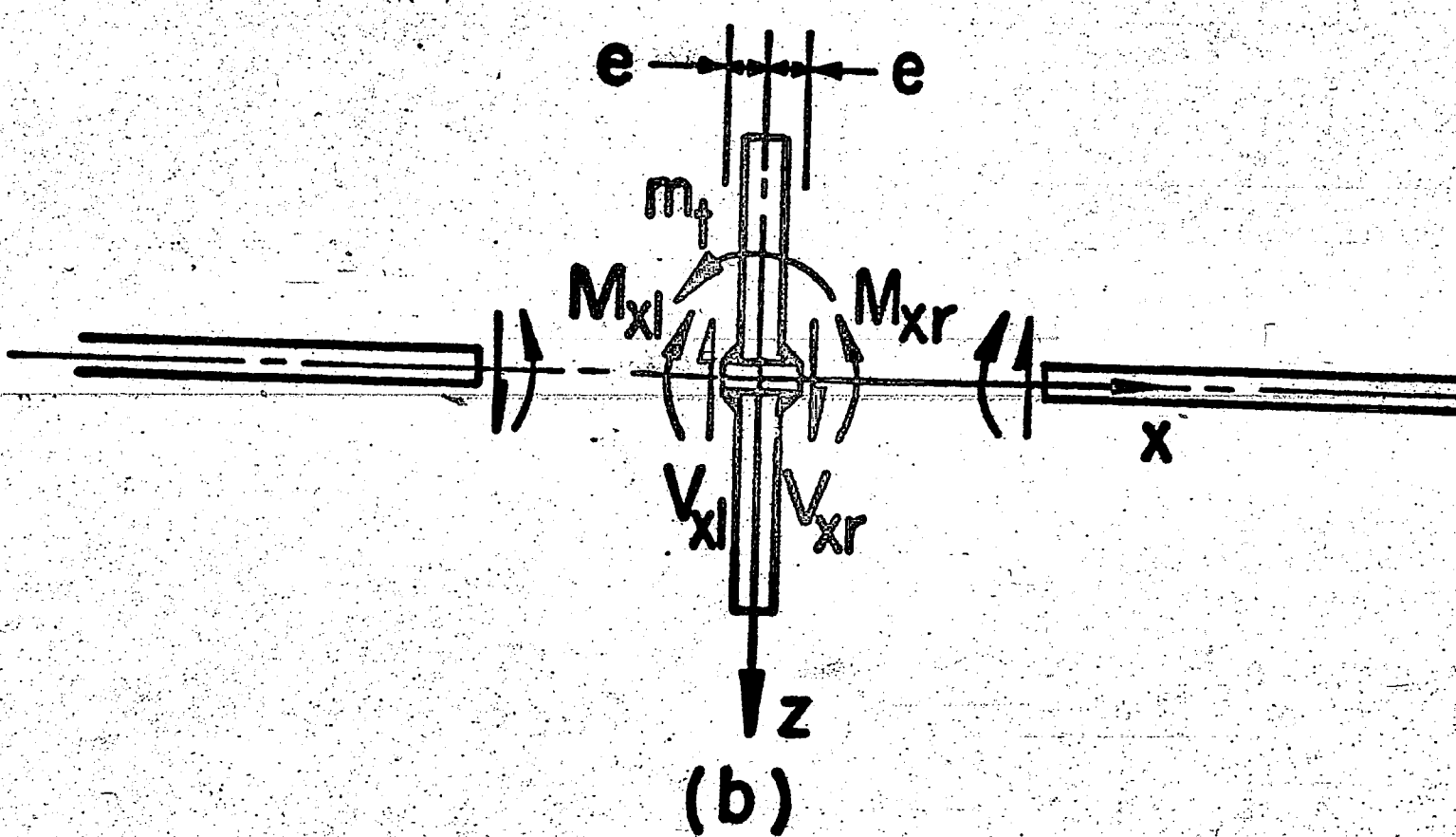


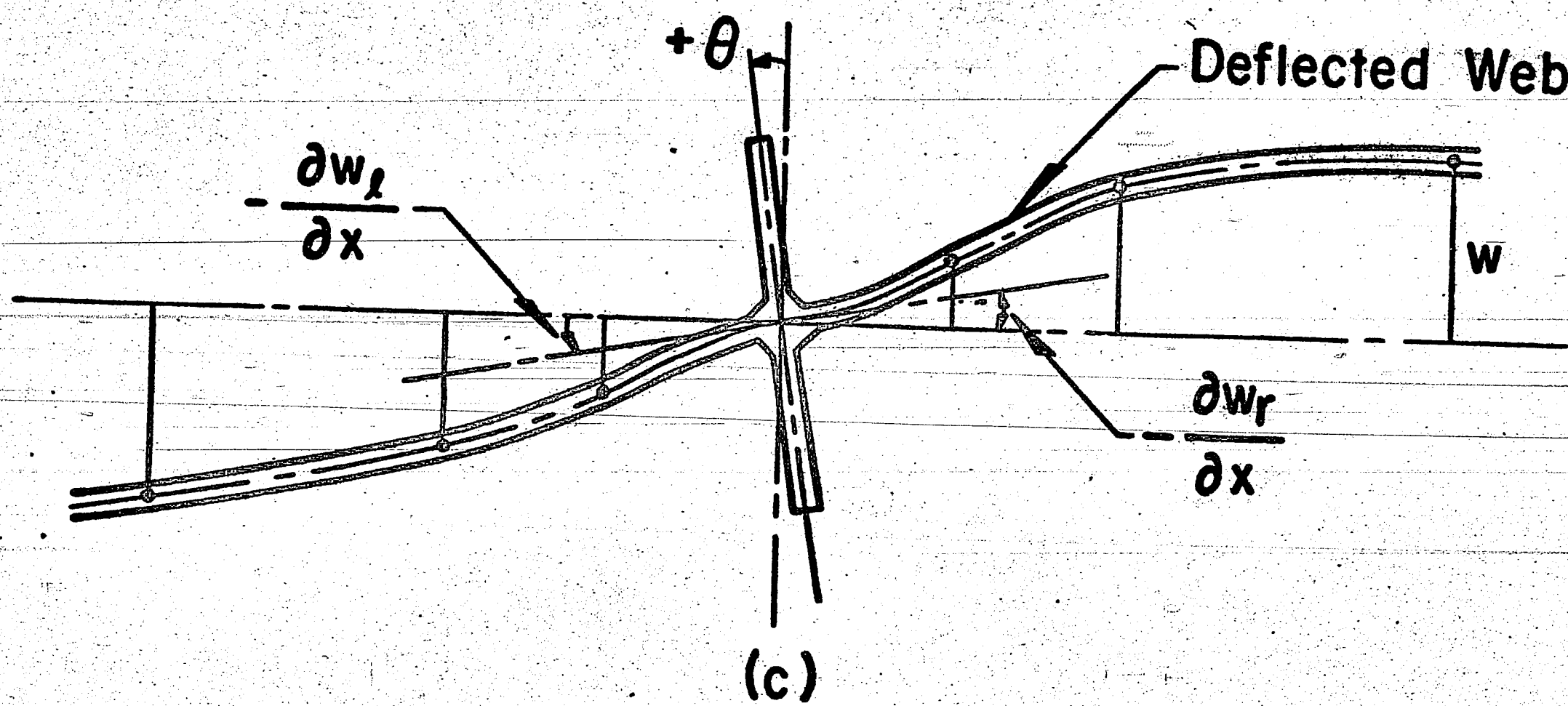
Fig. 2 Stress-Fatigue Life Relationship (S-N)



(a)



(b)



(c)

Fig. 3 Equilibrium and Compatibility Conditions  
for Stiffener-To-Web Junction

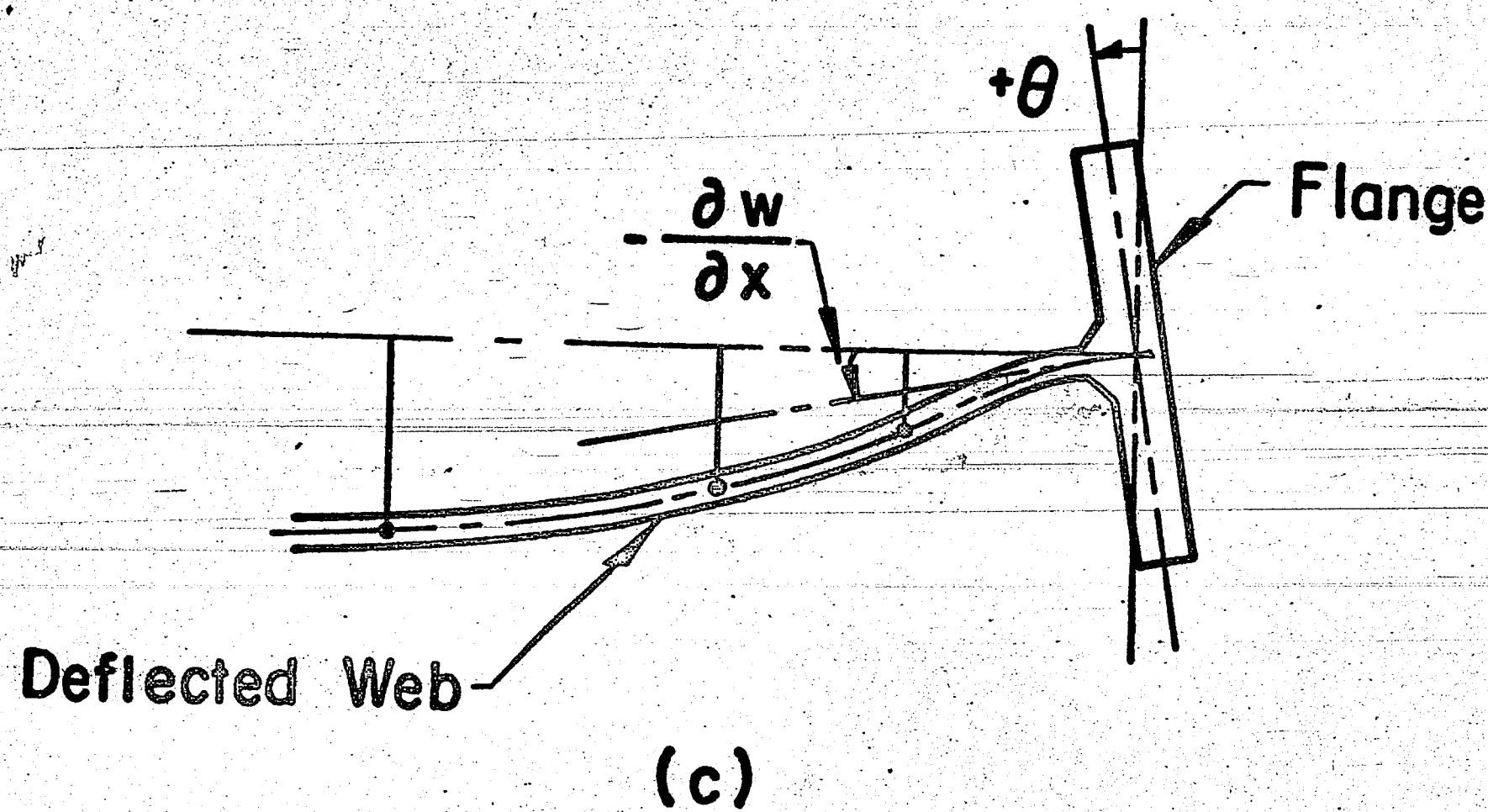
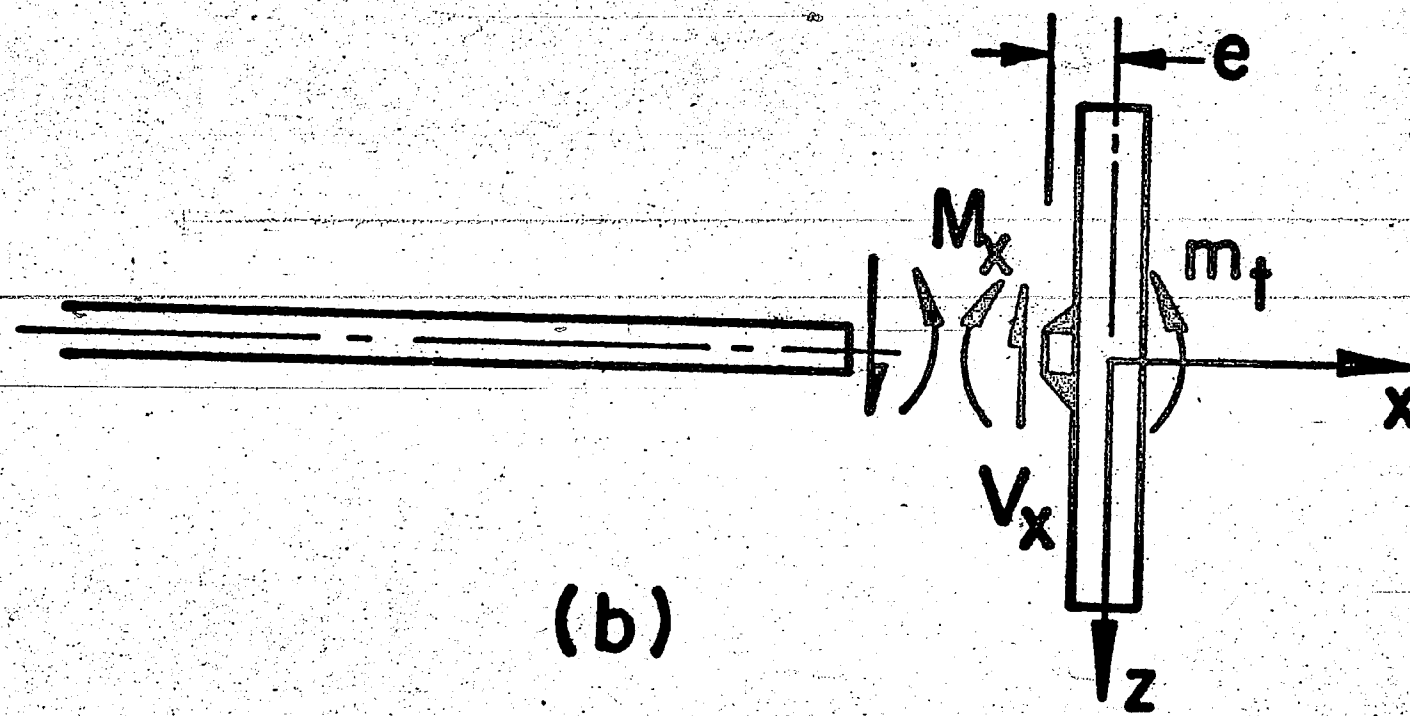
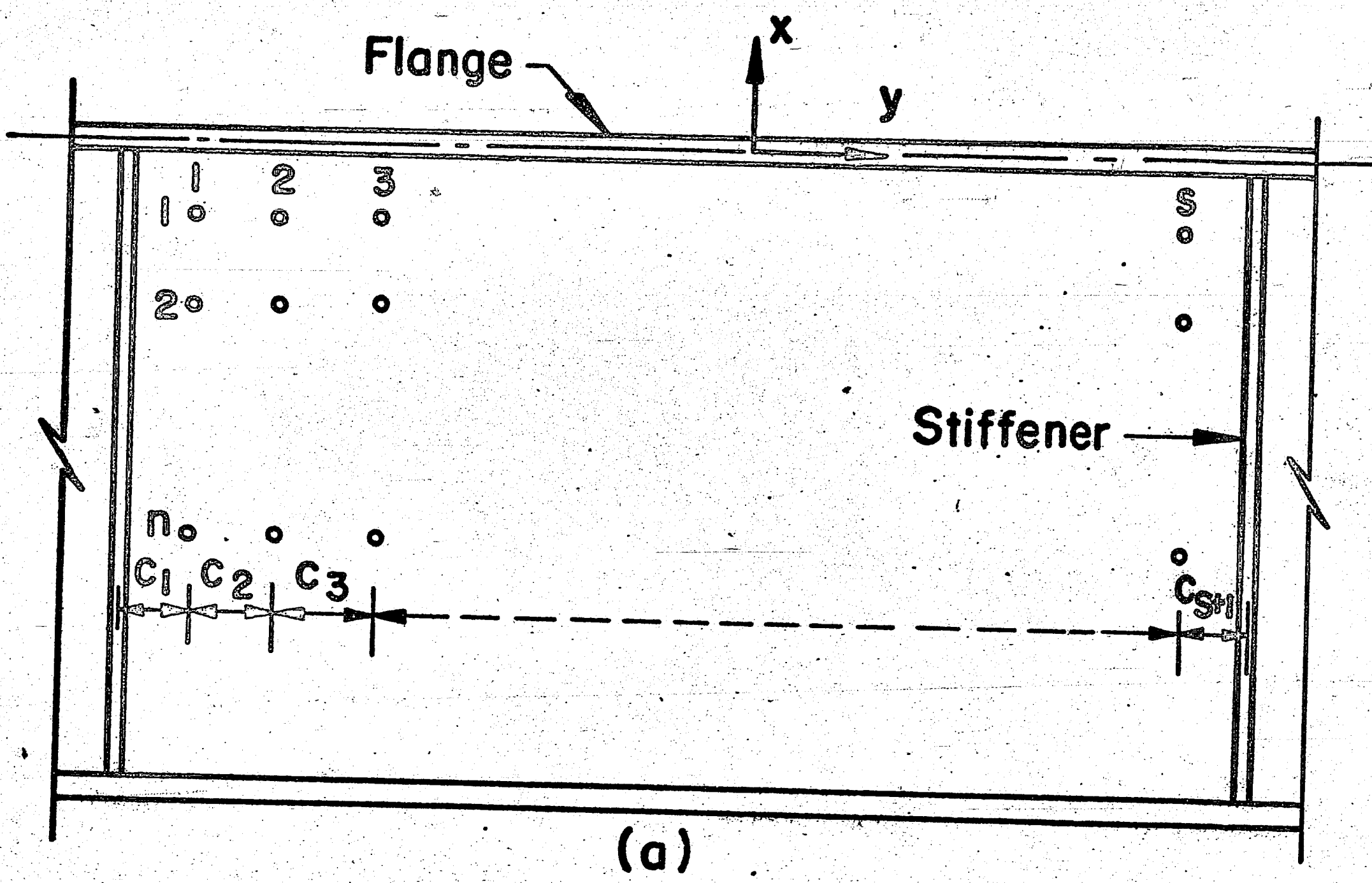


Fig. 4 Equilibrium and Compatibility Conditions  
for Flange-To-Web Junction

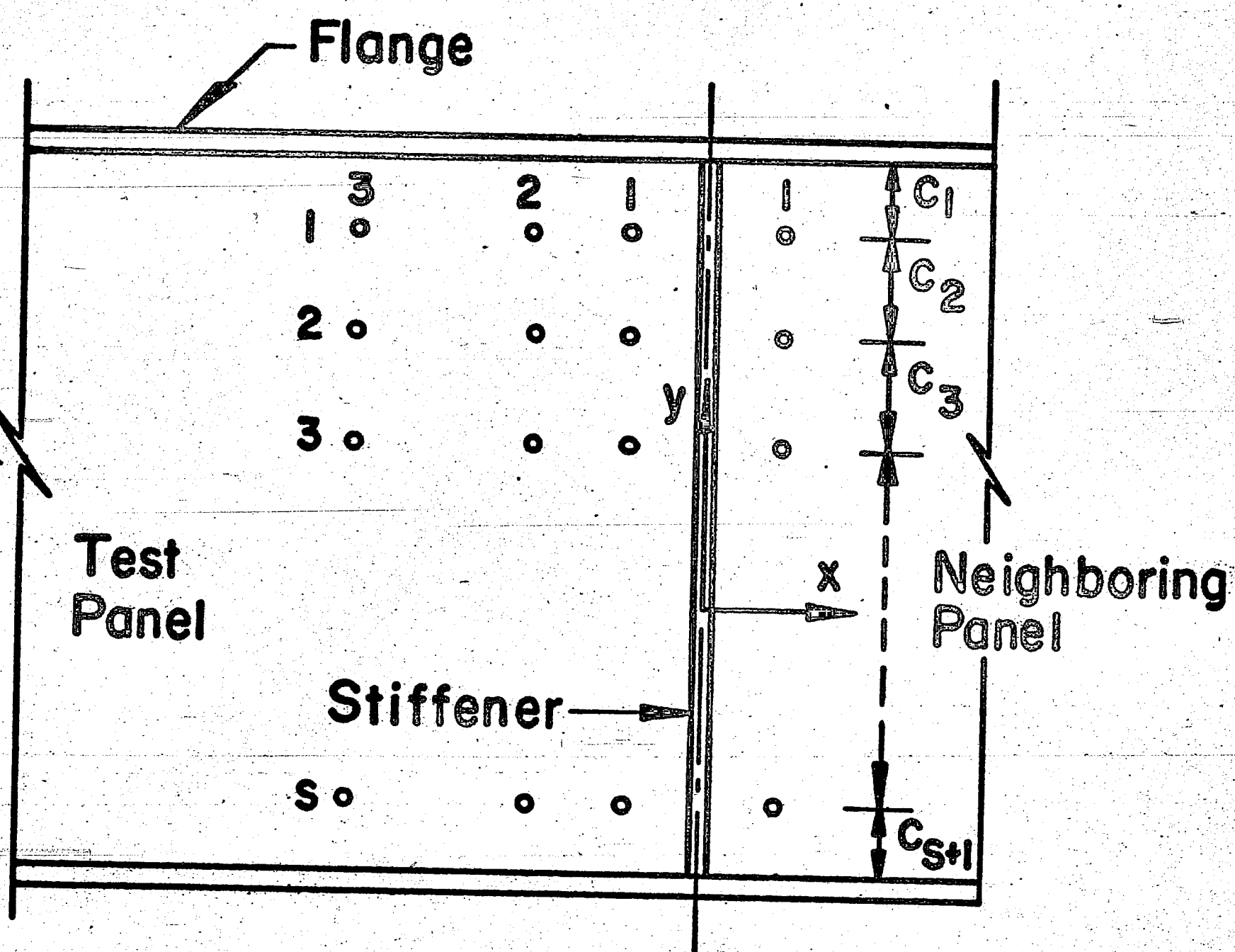


Fig. 5 Location of Web Deflection Measurements  
at Stiffener

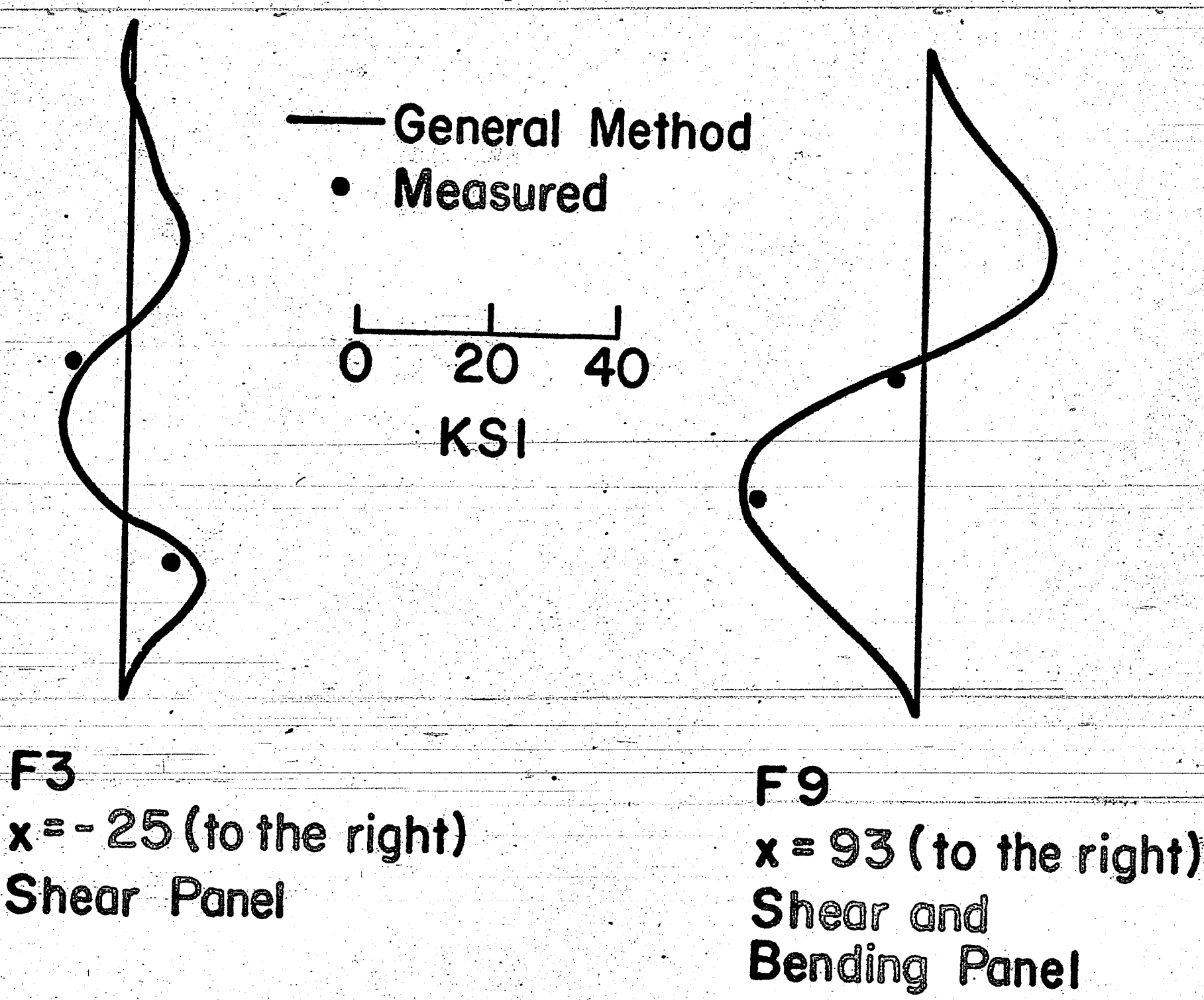


Fig. 6 Comparison Between Calculated and Measured  
Gage Stresses at Stiffener

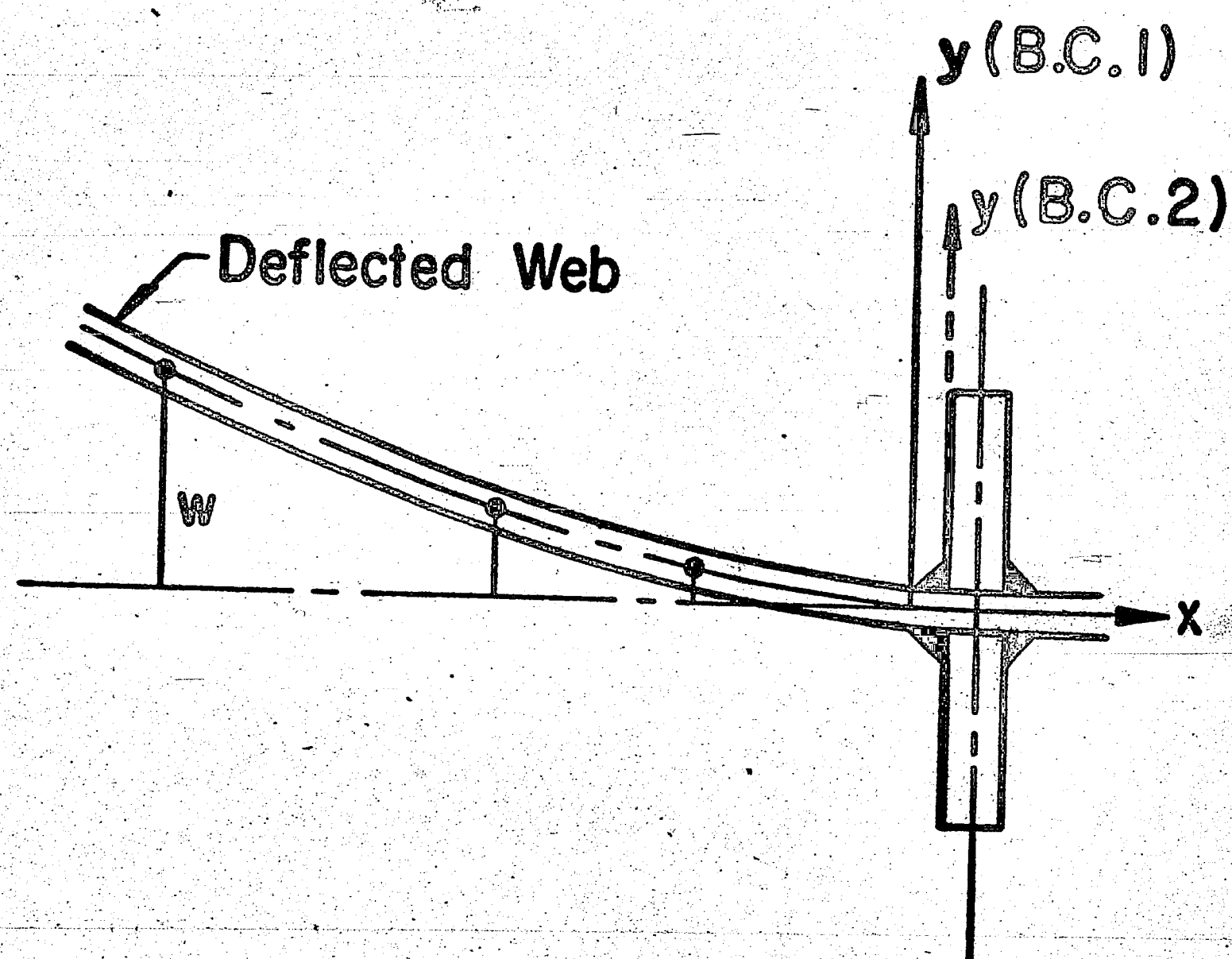


Fig. 7 Cantilever Models, B.C.1 and B.C.2

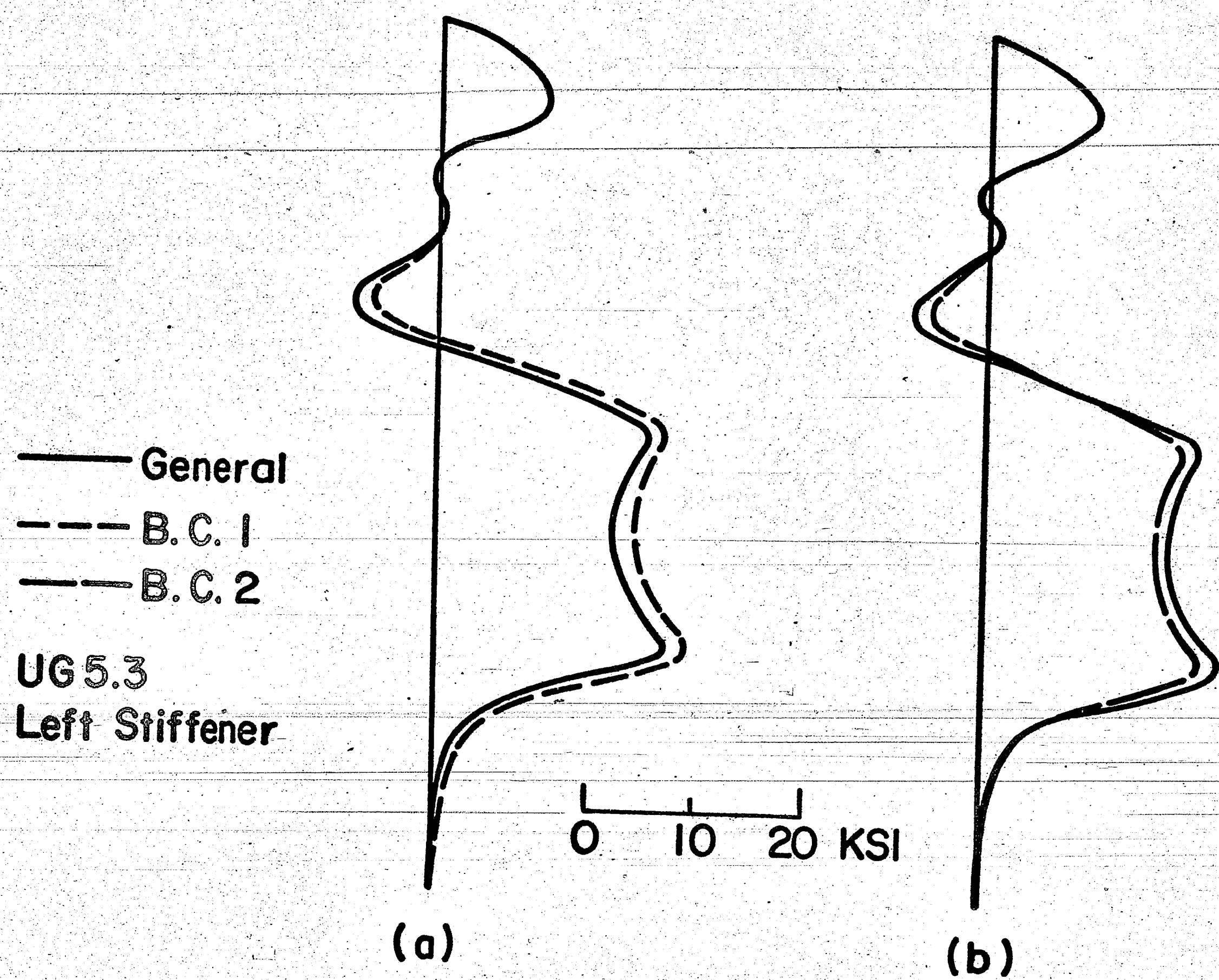


Fig. 8 Comparison of General Method with a) B.C.1  
and b) B.C.2 at Stiffener

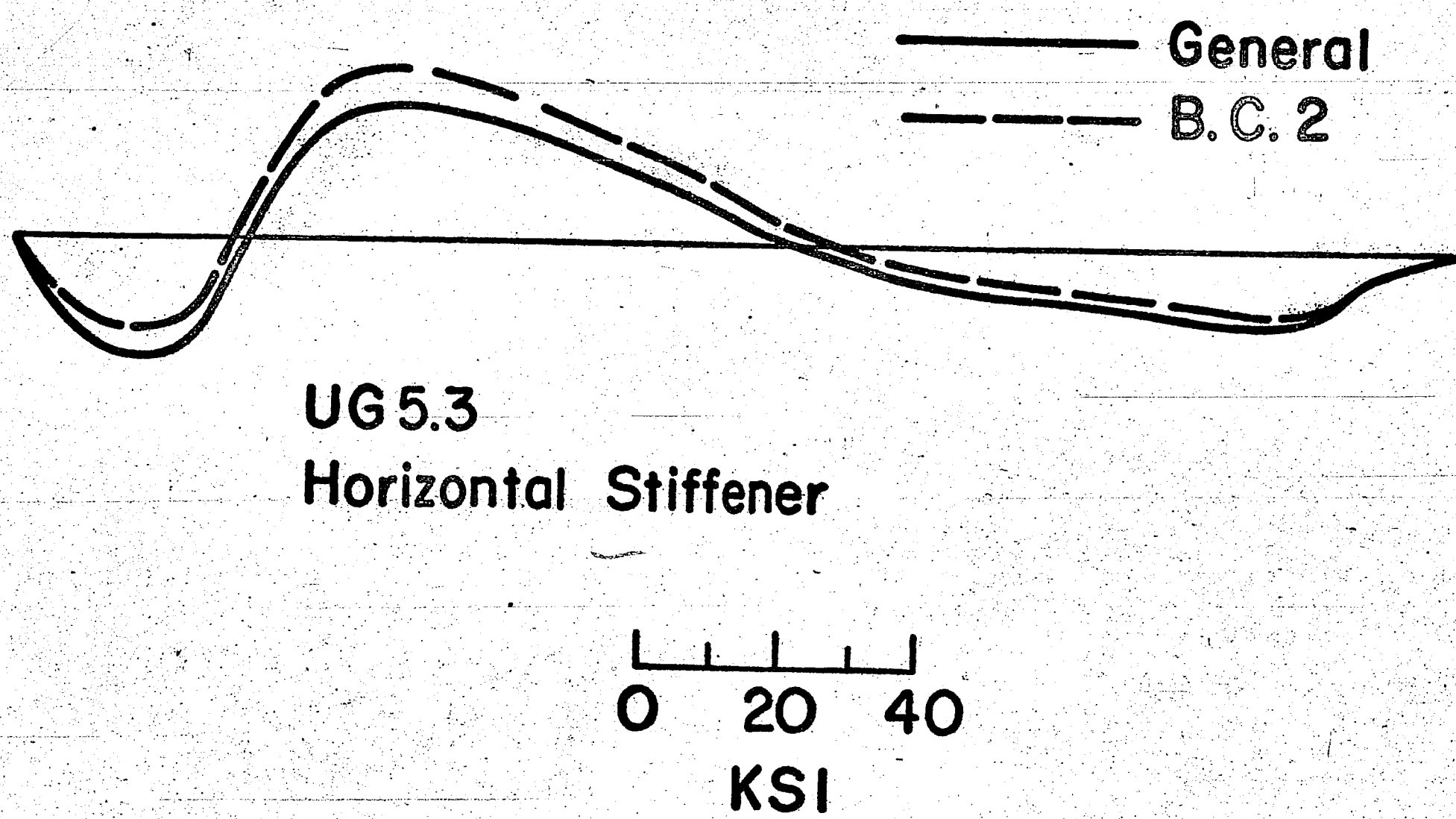


Fig. 9 Comparison of General Method with B.C. 2  
at Horizontal Stiffener

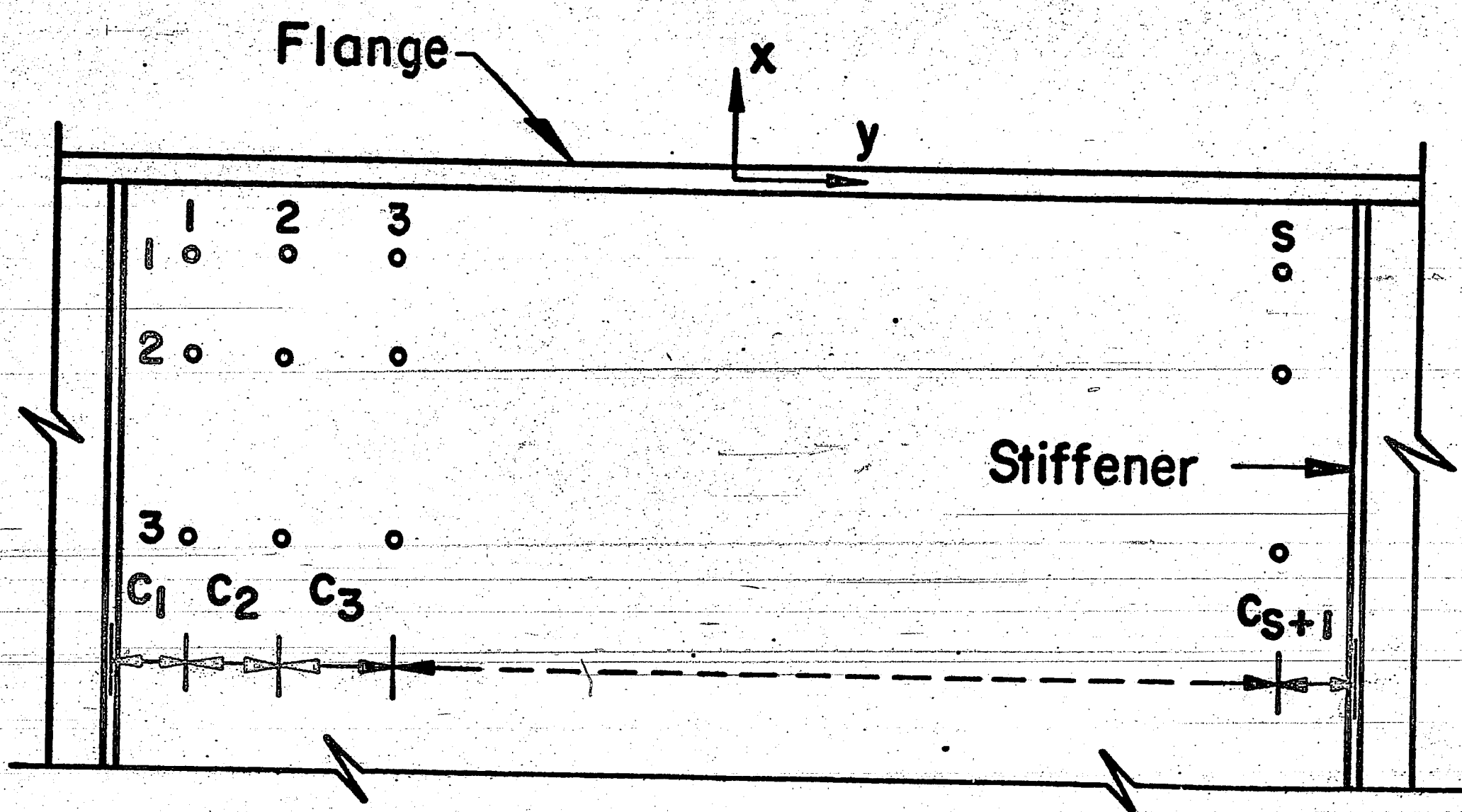


Fig. 10 Location of Web Deflection Measurements  
at Flanges

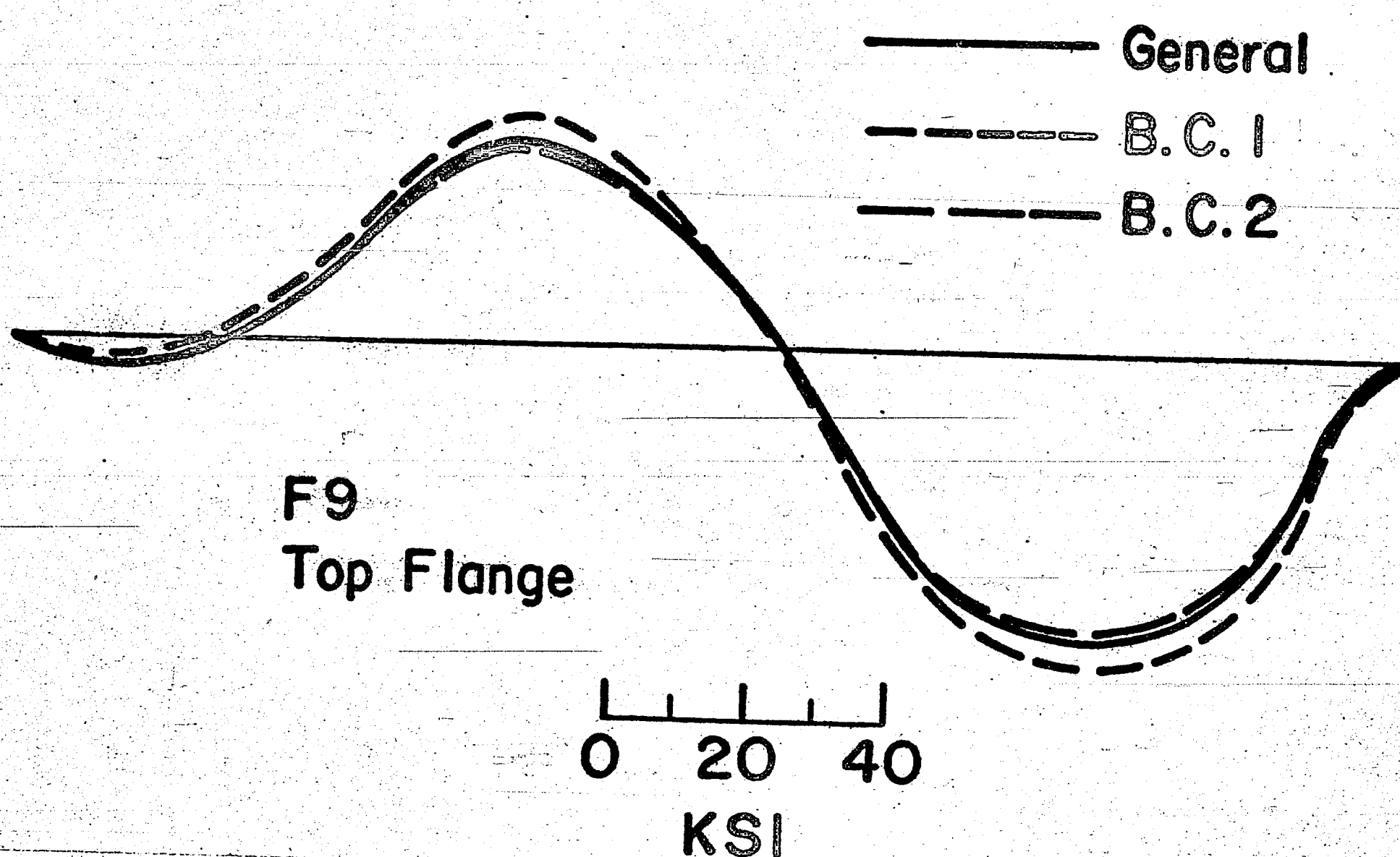


Fig. 11 Comparison of General Method with B.C.1 and B.C.2 at Flange

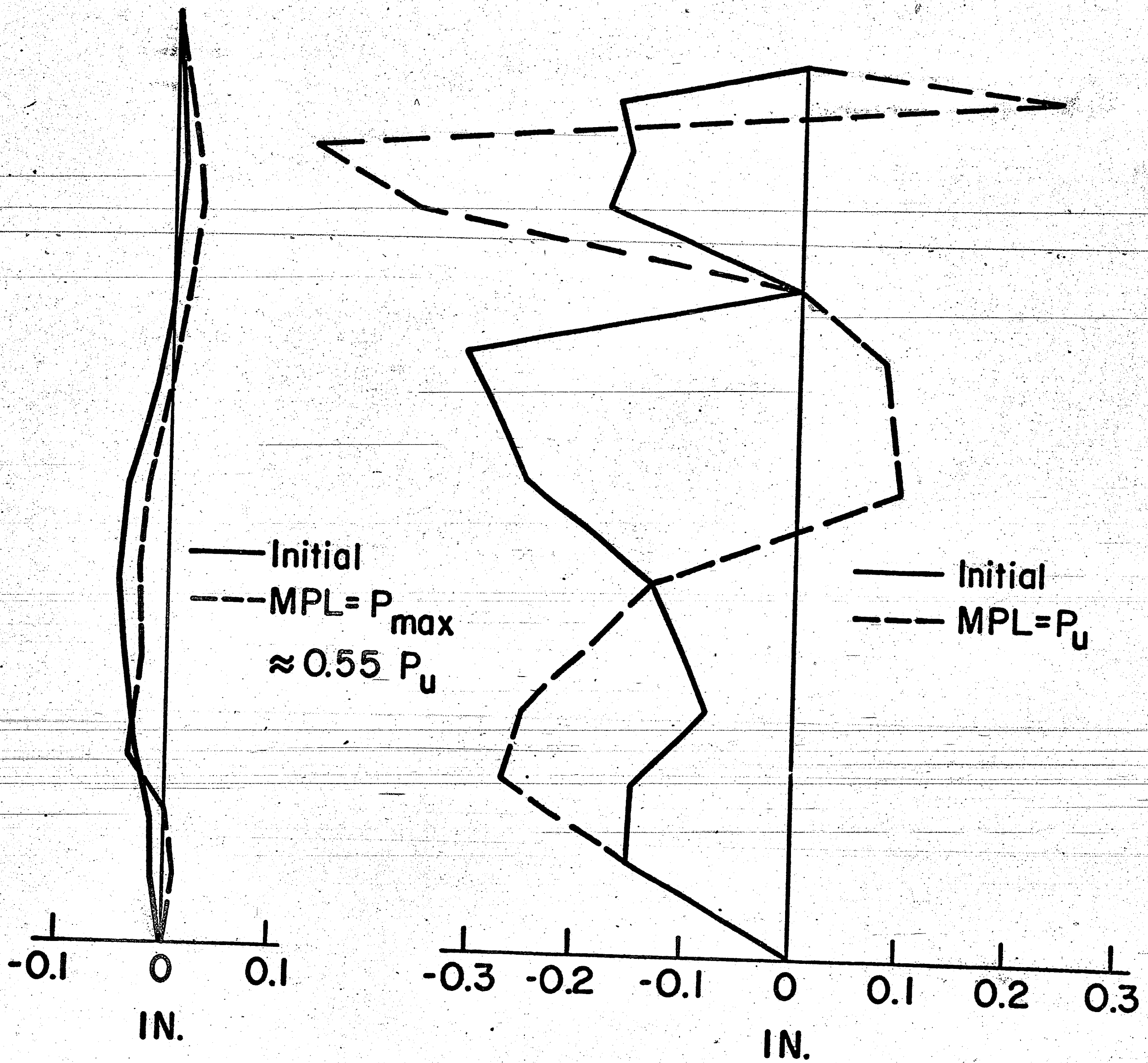


Fig. 12 Change in Deformation Pattern at Zero Load due to Maximum Past Load

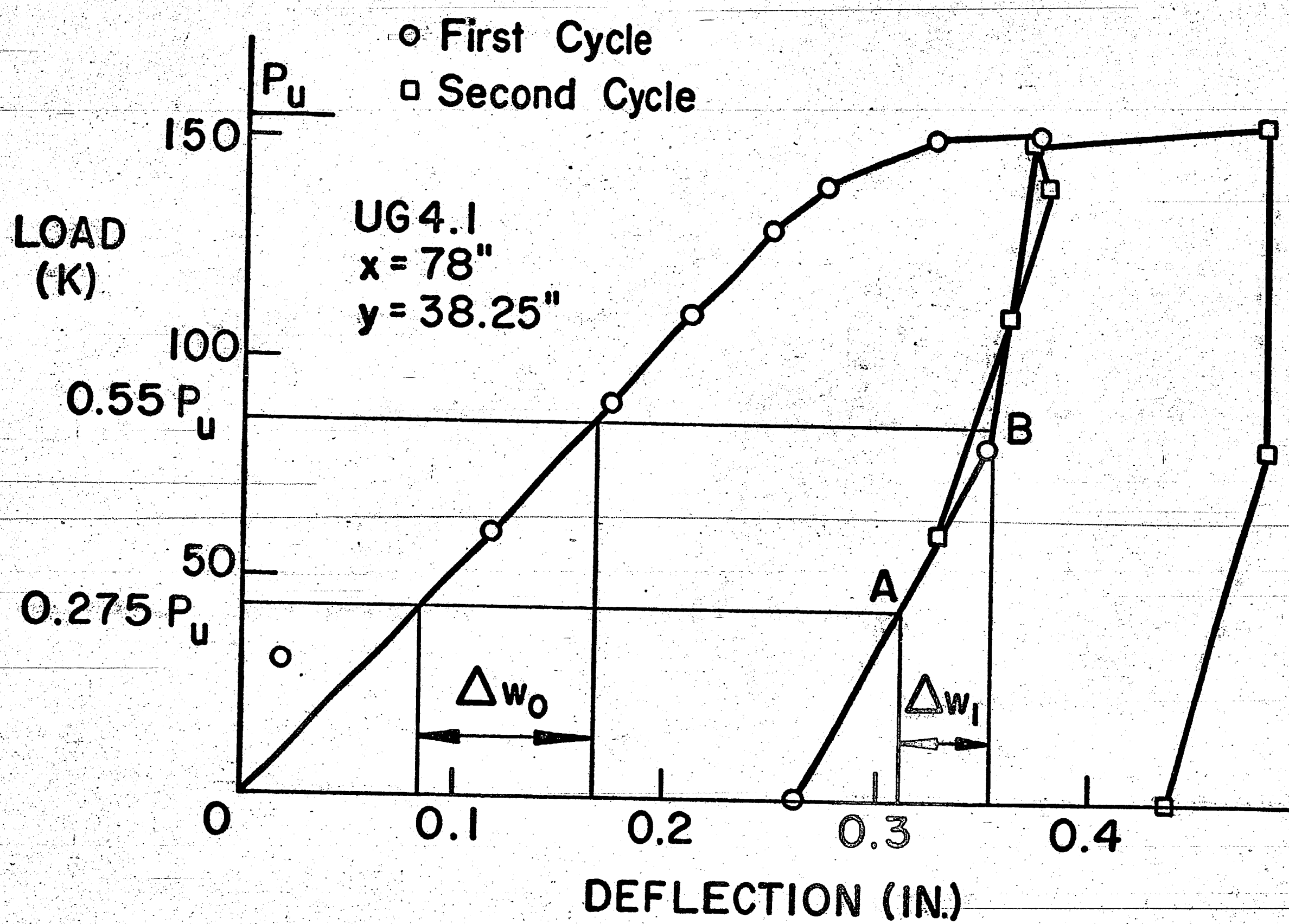
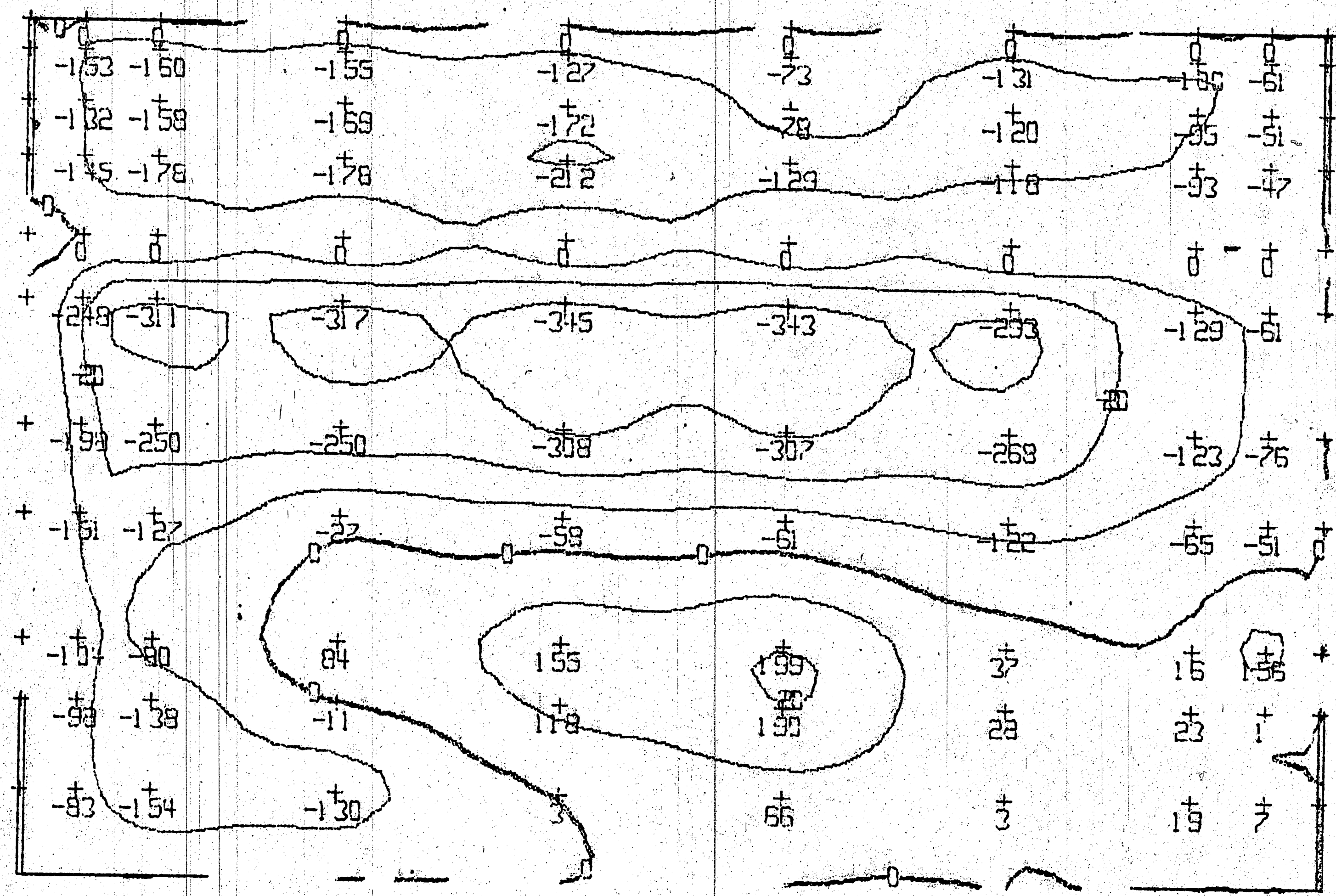


Fig. 13 Load-Deflection Plot of a Point on the Web



Deflections are in  $10^3$  inches

Fig. 14 Contour Plot of Initial Lateral Web Deflection of Panel UG 5.3

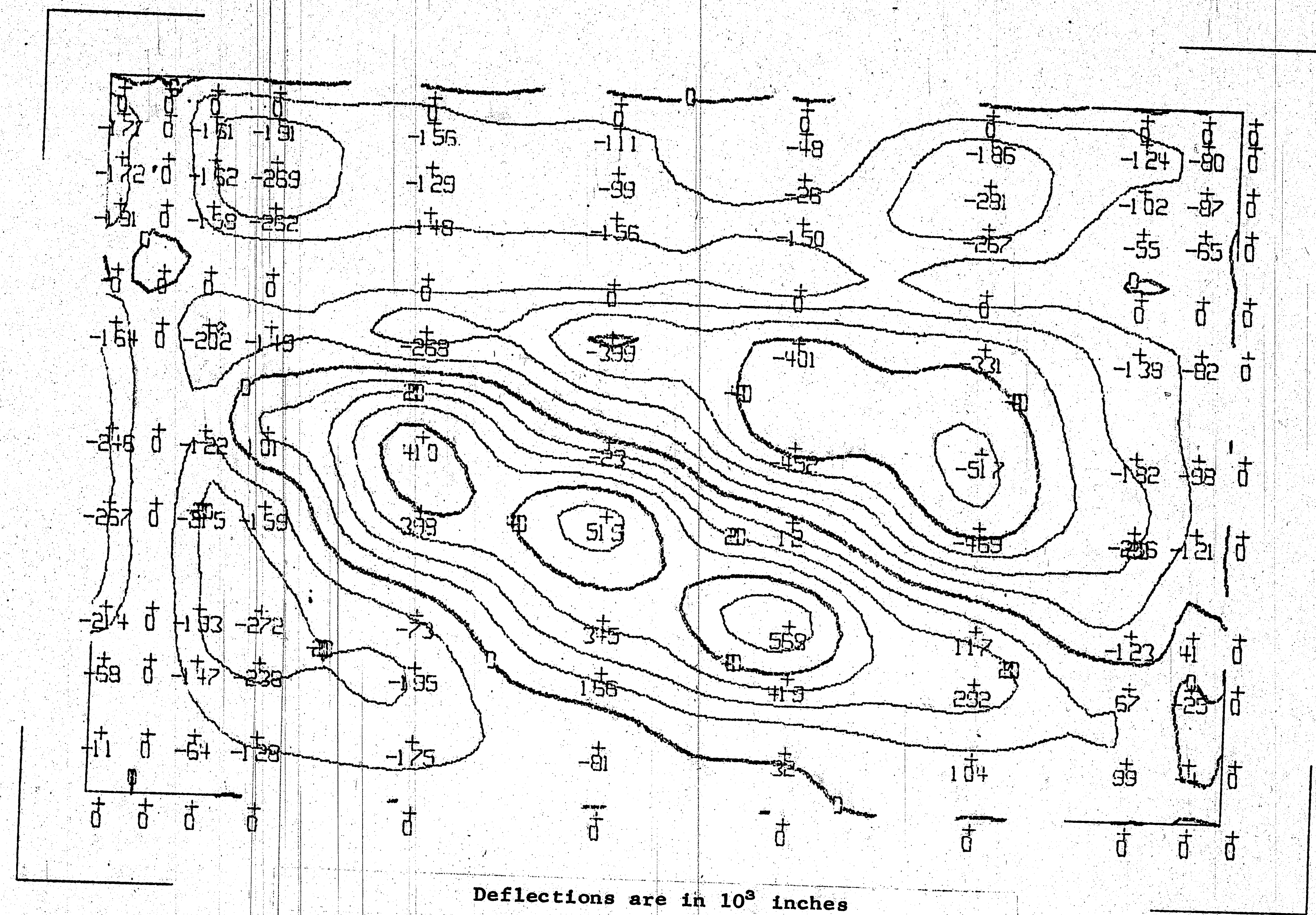
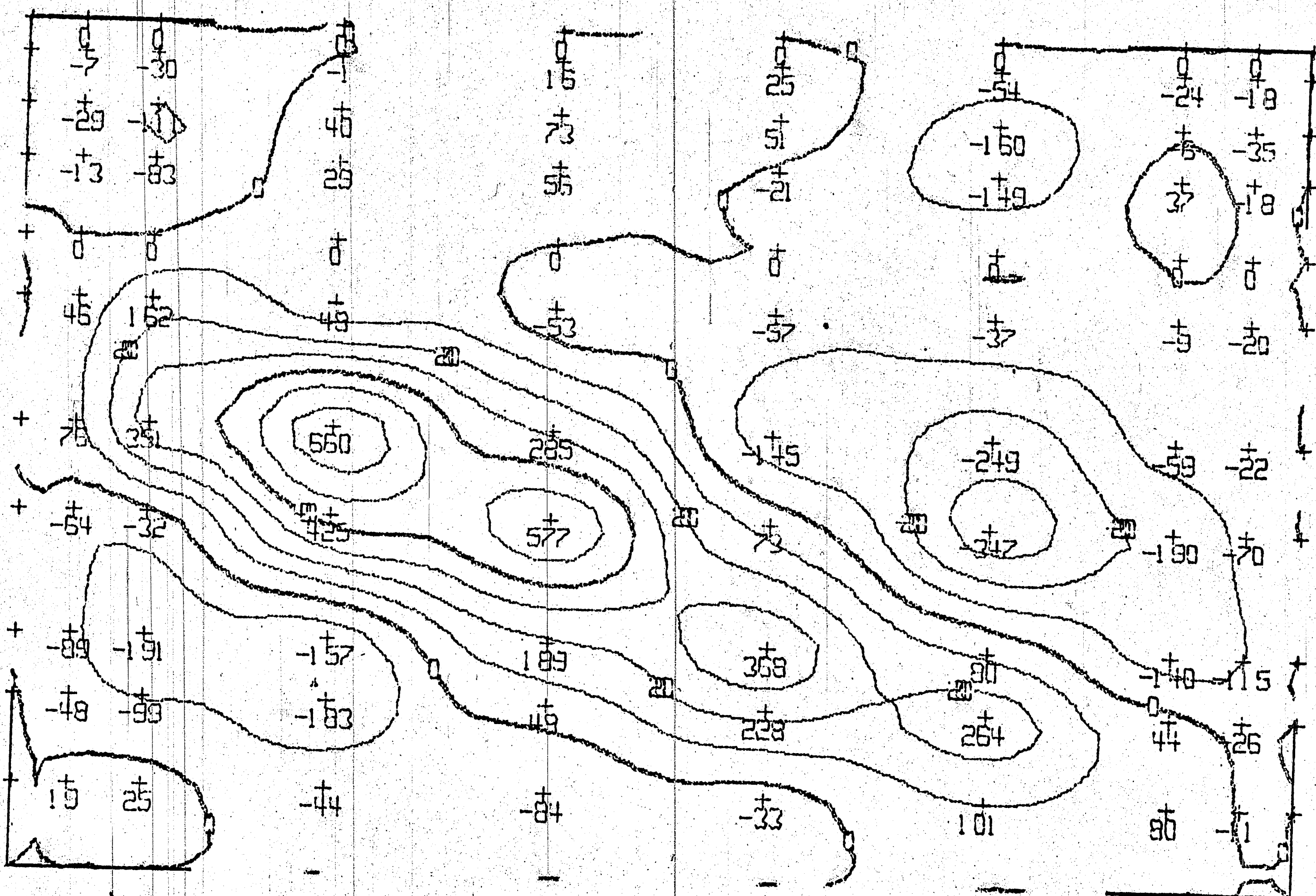


Fig. 15 Contour Plot of Lateral Web Deflection of Panel UG 5.3  
Subjected to 140k Load (73% of  $P_u$ )



Deflections are in  $10^3$  inches

Fig. 16 Contour Plot of the Change in Lateral Web Deflection  
of Panel UG 5.3 Due to 140<sup>k</sup> Loading

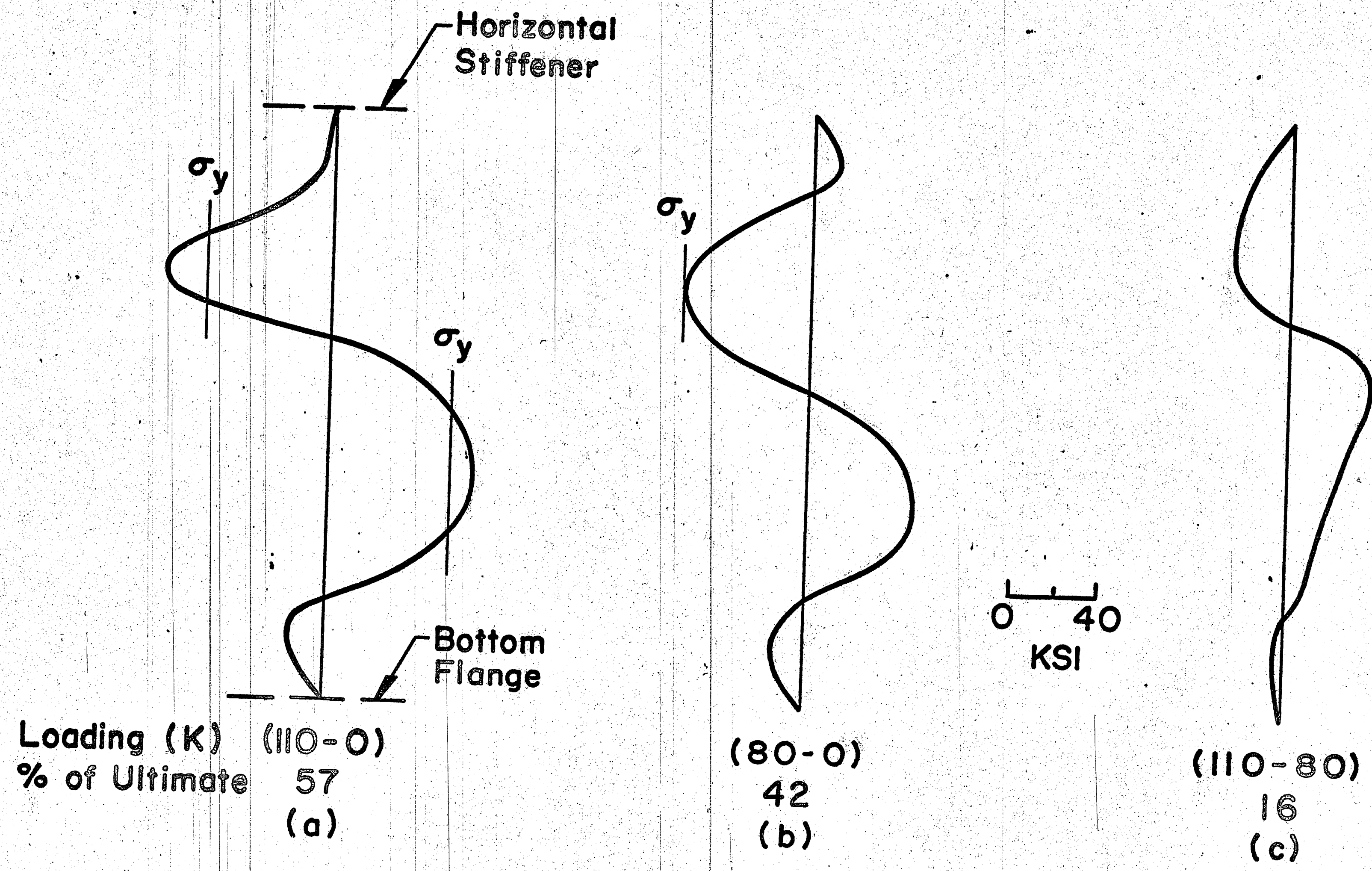


Fig. 17 Plate Bending Stresses at the Left Stiffener of Panel UG 5.3  
for Different Loading Ranges

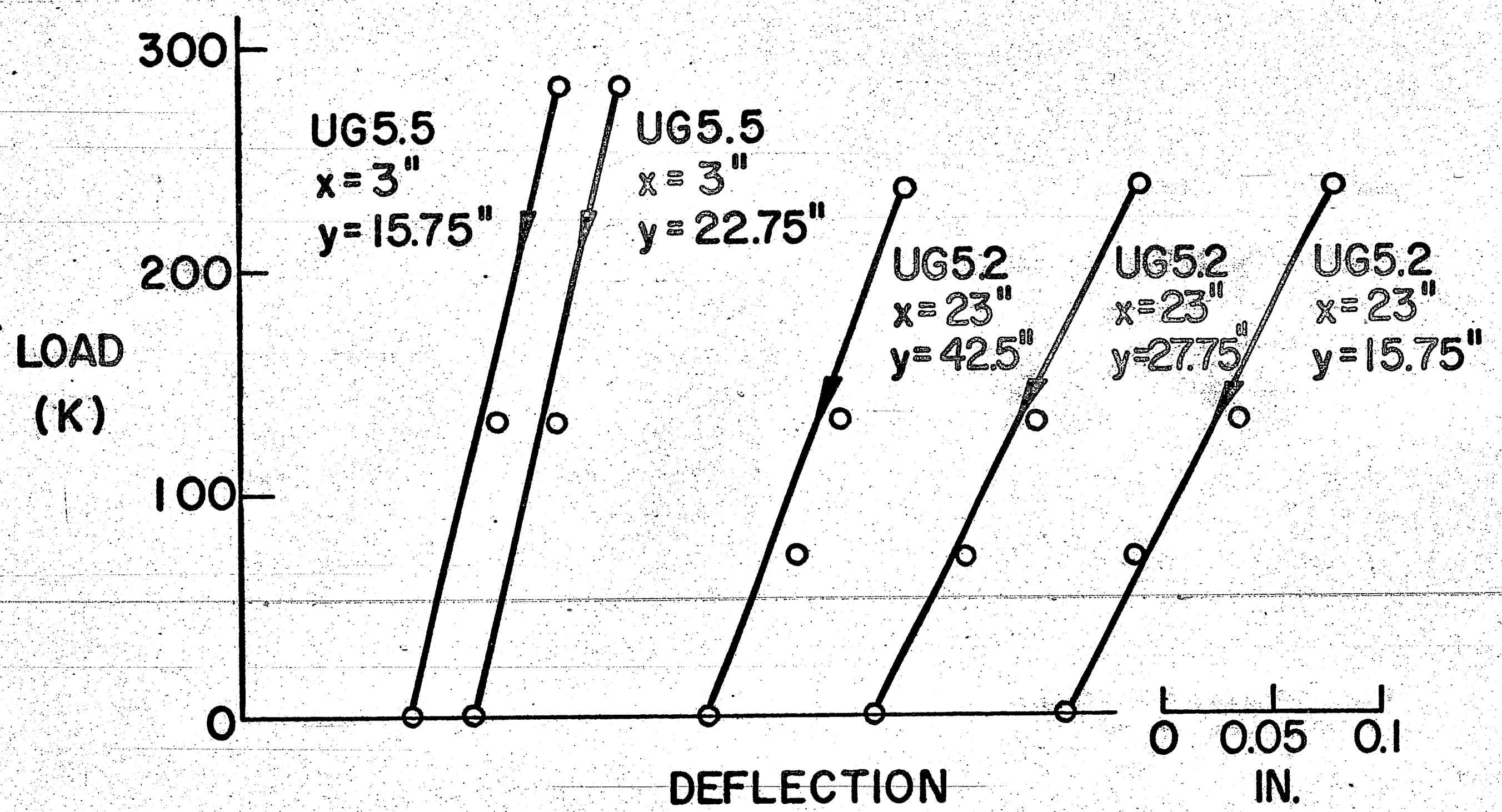


Fig. 18 Unloading Portion of Load-Deflection Plots  
of some Points on the Web

REFERENCES

1. Mueller, J. A. and Yen, B. T.  
GIRDER WEB BOUNDARY STRESSES AND FATIGUE, Bulletin No. 127,  
Welding Research Council, New York, January 1968.
2. Patterson, P. J., Corrado, J. A., Huang, J. S., and Yen, B. T.  
PROOF-TESTS OF TWO SLENDER-WEB WELDED PLATE GIRDERS,  
Fritz Engineering Laboratory Report No. 327.7, Lehigh  
University, May 1969.
3. Yen, B. T. and Mueller, J. A.  
FATIGUE TESTS OF LARGE-SIZE WELDED PLATE GIRDERS, Bulletin  
No. 118, Welding Research Council, New York, November 1966.
4. Yinh, J. and Toprac, A. A.  
STUDY ON FATIGUE OF HYBRID PLATE GIRDERS UNDER CONSTANT  
MOMENT, Research Report No. 96-3, The University of Texas,  
January 1969.
5. Goodpasture, D. W. and Stallmeyer, J. E.  
FATIGUE OF THIN-WEB STEEL GIRDERS, University of Illinois,  
April 1966 (Status Report to the Fatigue Committee of the  
Welding Research Council).
6. Schueler, W. and Ostapenko, A.  
STATIC TESTS ON UNSYMMETRICAL PLATE GIRDERS --- MAIN TEST  
SERIES, Fritz Engineering Laboratory Report No. 328.6,  
Lehigh University, September 1968.
7. Timoshenko, S. P. and Wolnowsky-Krieger, S.  
THEORY OF PLATES AND SHELLS, Second Edition, McGraw-Hill  
Book Company, New York, 1959.
8. Galambos, T. V.  
STRUCTURAL MEMBER AND FRAMES, Prentice-Hall, Englewood  
Cliffs, New Jersey, 1968.

VIITA

Siamak Parsanejad was born on November 20, 1941 in Tehran, Iran as the second child of Alimohammad and Badrozzaman Parsanejad. He is married to Fattaneh (Rezvan) and has one child, Ali.

He received his high school diploma from Hadaf High School in Iran and afterwards studied architecture for three years at the University of Tehran, Iran.

He completed his first two years of engineering education in Yuba College, Marysville, California and received there an academic award. He received his Bachelor of Science Degree in Civil Engineering in January 1968 from San Jose State College, San Jose, California, where he was awarded the citation as Dean's Scholar. From February to September 1968, he worked as a junior structural designer for Modulux Inc., Newark, California.

In the fall of 1968, he entered graduate school in the Department of Civil Engineering, Lehigh University pursuing a Master of Science Degree and worked as a half-time research assistant in Fritz Engineering Laboratory.